UNIVERSITÉ DU QUÉBEC À MONTRÉAL

EFFET DES SCÉNARIOS DE MITIGATION DE L'ILÔT DE CHALEUR URBAIN SUR LA PRÉCIPITATION ET LA TEMPÉRATURE À MONTRÉAL, CANADA : DEUX ÉTUDES DE CAS

MÉMOIRE

PRÉSENTÉ(E)

COMME EXIGENCE PARTIELLE

DE LA MAÎTRISE EN SCIENCES DE L'ATMOSPHÈRE

PAR

AUDREY LAUER

JUIN 2023

REMERCIEMENTS

Je tiens à remercier toutes les personnes qui m'ont aidée dans mon projet de recherche et dans la rédaction de ce mémoire.

Je voudrais tout d'abord remercier mon directeur de recherche, le professeur Francesco S.R. Pausata pour son soutien et son encadrement tout au long du projet, ainsi que de m'avoir encouragée à écrire un premier article scientifique. Un énorme merci à Sylvie Leroyer, co-directrice de recherche, d'avoir permis la réalisation du projet avec les infrasctructures d'Environnement et Changement climatique Canada, ainsi que pour tout le temps qu'elle a consacré à m'aider, me soutenir et m'encourager dans ma maîtrise. Je remercie également Daniel Argüeso, qui a pris le temps de me conseiller dans l'analyse des résultats et la rédaction de mon mémoire. À vous trois, merci pour votre patience, vos conseils et vos commentaires.

Enfin, je remercie du fond du cœur ma famille et amis pour leur soutien moral bien nécessaire tout au long de ma maîtrise. Merci Frédérique, merci pour ton soutien inconditionnel.

TABLE DES MATIÈRES

LISTE DES FIGURES

LISTE DES TABLEAUX

LISTE DES ABRÉVIATIONS, DES SIGLES ET DES ACRONYMES

ALB	Expérience où l'albédo des surfaces urbaines est augmenté (Experiment in which the albedo of the urban surfaces is increased)
CaLDAS	Système canadien d'assimilation de surface (Canadian Land Data Assimilation System)
CaPA	Analyse de précipitation canadienne (Canadian Precipitation Analysis)
CaPA-HRDPA	(High-Resolution Deterministic Precipitation Analysis)
CAPE	Énergie potentielle de convection disponible (Convective available potential energy)
CCN	Noyau de condensation (Cloud condensation nuclei)
CIN	Énergie d'inhibition de la convection (Convective inhibition)
CTL	Expérience de contrôle (control experiment)
ECCC	Environnement et changements climatiques Canada (Environment and Climate Change Canada)
GEM	Modèle global environnemental multiéchelles (Global Environmental Multiscale Model)
HRDPS	Système à haute résolution de prévision déterministe (High-Resolution Deterministic Prediction System)
ISBA	Modèle *Interaction between Soil-Biosphere-Atmosphere* (Interaction between Soil-Biosphere-Atmosphere)
NOURB	Expérience sans aires urbaines (Experiment without any urban areas)
NWP	Prévision numérique du temps (Numerical weather prediction)
TEB	Modèle *Town Energy Balance* (Town Energy Balance)
ICU/UHI	Ilot de chaleur urbain (Urban heat island)

VEG	Expérience où de la végétation basse est ajoutée dans la ville (Ein which urban vegetation is enhanced)

LISTE DES SYMBOLES ET DES UNITÉS

PR	Précipitation (Precipitation)
TD	Température du point de rosée (Dew-point temperature)
TT	Température (Temperature)

RÉSUMÉ

Nous utilisons des experiences de prévision numérique du temps à haute résolution avec le modèle global environnemental multiéchelles (GEM) afin d'étudier l'effet de la surface sur la température, le confort thermique ainsi que la précipitation sur la région de Montréal (Canada). Nous étudions deux différents évènements de précipitation intense suivant des températures élevées durant les 2-3 jours précédant la pluie : le premier est un système à grande échelle traversant la région durant la nuit, et le deuxième, une ligne de grain qui croise la ville l'après-midi. Notre modèle est performant et représente adéquatement la température de l'air, la température du point de rosée et la précipitation lors des deux évènements étudiés, malgré que les systèmes semblent être légèrement bloqués en amont de la zone urbaine. Des expériences de sensibilité à l'occupation de la surface sont effectuées. Le remplacement de toutes les surfaces urbaines par de la végétation basse conduit à l'amélioration du confort thermique en diminuant l'indice de chaleur de 2-6°C. L'augmentation de l'albédo des surfaces urbaines mène à une amélioration du confort de 0.5-1°C dans la région, tandis que lors de l'ajout de végétation basse en ville, une amélioration du confort jusqu'à 0.5°C est relevée dans les régions urbaines denses seulement. En ce qui concerne la précipitation, le signal de la ville est seulement visible dans le cas de la ligne de grain, où le patron de précipitation est différent quand la ville est présente et quand elle est retirée numériquement. Ces résultats peuvent supporter des choix de design urbains futurs afin de réduire l'effet de l'ilôt de chaleur urbain.

Mots clés : simulations numériques, îlot de chaleur urbain, précipitation, température, confort

ABSTRACT

High-resolution numerical weather prediction experiments using the Global Environmental Multiscale (GEM) model are used to investigate the effect of the urban land-use on temperature, comfort and rainfall over the Montreal (Canada) area. We focus on two different events of high temperatures lasting 2-3 days followed by intense rainfall: one is a large-scale synoptic system that crosses Montreal during nighttime and the other is an afternoon squall line. Our model shows an overall good performance in adequately capturing the surface air temperature, dew-point temperature and rainfall during the events, although the precipitation pattern seems to be slightly blocked upwind of the city. Sensitivity experiments with different land use scenarios were conducted. Replacing all urban surfaces by low vegetation showed an increase of human comfort, lowering the heat index by 2-6°C. Increasing the albedo of urban surfaces leads to an improvement of comfort of 0.5-1°C, whereas adding street-level low vegetation had an improvement of comfort of up to 0.5°C in the downtown area. With respect to precipitation, significant differences are only seen for the squall line event, for which removing the city modifies the precipitation pattern. These findings could support future design choices to mitigate the urban heat island.

Keywords : numerical simulation, urban heat island, precipitation, temperature, comfort

INTRODUCTION

Bien que les villes n'occupent qu'une petite fraction de la surface de la Terre, plus de la moitié de la population mondiale habite dans celles-ci, et cette proportion risque d'augmenter significativement dans les prochaines décennies (*World Urbanization Prospects*, 2019). Les villes ont un impact sur l'environnement local puisqu'elles sont bâties selon une géométrie particulière et avec des matériaux différents de ceux qu'on retrouve dans la nature. Les structures urbaines viennent notamment modifier les échanges de chaleur et d'humidité entre la surface et l'atmosphère, ainsi qu'influencer les vents de surface. Il est crucial de bien comprendre ces interactions afin d'identifier et de réduire les risques auxquels est exposée la population urbaine.

Les températures de surface des zones urbaines sont plus élevées que celles des milieux ruraux avoisinants (Mills, 2008), phénomène qui est bien observé et documenté depuis le début du 19e siècle et que l'on appelle îlot de chaleur urbain (ICU) (Oke, 1982; Stewart, 2011). Les matériaux utilisés dans la construction des villes ont une faible réflectance, sont de bons conducteurs thermiques et ont une plus grande capacité thermique. Ainsi, ils absorbent et emmagasinent plus efficacement que les matériaux naturels, les flux de radiation et la chaleur, qui sont par la suite relâchés durant la nuit sous forme de chaleur sensible et de rayonnement infrarouge. Cet effet est accentué par la géométrie urbaine. Le rayonnement solaire est réfléchi à plusieurs reprises entre les routes et les bâtiments, augmentant ainsi la probabilité d'être absorbé par le tissu urbain (Oke et al., 2017). Aussi, les surfaces urbaines sont imperméables, ce qui altère le bilan hydrologique en réduisant l'infiltration, en réduisant les périodes d'évaporation et en augmentant l'écoulement de surface. Il y a également moins de végétation dans les milieux urbains que dans les milieux ruraux, donc l'évapotranspiration par les plantes est peu importante en ville. Ceci a pour effet de réduire le refroidissement de l'air dû à l'évaporation et, ainsi, la majorité des échanges de chaleur entre la surface et l'atmosphère se produit sous forme de flux de chaleur sensible. De plus, les zones urbaines réduisent le vent de surface, ce qui accentue l'emmagasinement de chaleur dans la ville (He et al., 2020; Oke et al., 2017). Finalement, des sources anthropogéniques de chaleur, comme les bâtiments et les voitures, ainsi que la pollution atmosphérique sont plus importantes dans les villes et modifient le bilan énergétique (Oke et al., 2017).

Les planificateur·rice·s des zones urbaines cherchent à adopter différentes stratégies dans le but de réduire l'intensité de l'ICU et ses effets sur la population. Deux stratégies fréquemment employées sont

l'ajout d'infrastructures vertes telles que des toits verts, des parcs et des arbres (Berardi et al., 2020; Krayenhoff et al., 2020; Lee et al., 2016; J. Yang et al., 2016) et l'augmentation de la réflectivité des surfaces urbaines (Krayenhoff & Voogt, 2010; Taha et al., 1988; Taleghani & Berardi, 2018; F. Yang et al., 2011). Tout d'abord, l'ajout de végétation dans les milieux urbains tend à réduire la température de surface de l'air en augmentant l'évapotranspiration et, dans les cas où les surfaces urbaines sont remplacées par de la végétation (parcs, toits verts, etc.), le processus d'emmagasinage de chaleur durant le jour et de relâchement la nuit est moins important. Malgré cette réduction de la température de surface, la végétation ajoute de la vapeur d'eau dans l'air, ce qui peut potentiellement réduire le confort ressenti par les habitant·e·s de la ville. Plusieurs études ont toutefois démontré que, globalement, l'ajout d'infrastructures vertes dans une ville réduit le stress thermique (Broadbent et al., 2018; Lee et al., 2016). De plus, le type de végétation (c.-à-d. de la végétation haute ou basse) qui est ajoutée et son emplacement dans le canyon urbain peuvent avoir un effet différent sur le confort thermique. Par exemple, les arbres interagissent avec la radiation en créant des zones ombragées à la surface et sont donc plus efficaces à améliorer le confort (Krayenhoff et al., 2020). Puis, l'augmentation de l'albédo et de la réflectivité des surfaces urbaines diminue la température de surface de l'air durant le jour, puisqu'elles réfléchissent davantage le rayonnement solaire, alors que l'impact durant la nuit est négligeable (Taleghani & Berardi, 2018; F. Yang et al., 2011; J. Yang et al., 2016). Finalement, l'efficacité de ces stratégies dépend grandement de la localisation géographique, de la taille et de la composition de la ville. De plus, l'intensité de l'ICU est typiquement plus grande la nuit que le jour, malgré que l'impact le plus important sur la population urbaine est durant le jour (Martilli et al., 2020). Ainsi, les stratégies de reduction de l'ICU les plus efficaces sont celles qui augmentent le comfort thermique durant le jour, plutôt que simplement l'intensité de l'ICU global.

Plus récemment, les études ont montré que les villes ont un large impact sur la précipitation. En regroupant et en résumant des études d'observation et de modélisation, Liu & Niyogi (2019) montrent une augmentation des quantités de précipitation de 16% au-dessus des villes et de 18% à 20-50 km en aval de celles-ci (Liu & Niyogi, 2019). Bien que les processus physiques qui influencent les paramètres de surface (température et humidité) sont bien compris, la compréhension de ceux influençant la précipitation urbaine évolue encore. Plusieurs facteurs complexes influencent les systèmes de précipitation, tels que les mouvements synoptiques des systèmes et la microphysique des nuages : il est donc difficile d'isoler l'effet potentiel de la ville. Néanmoins, les mécanismes les plus importants sont les suivants.

- Une augmentation de la convergence dans les bas niveaux due à la rugosité plus élevée des villes peut impacter la convection au-dessus de celles-ci (Bornstein & Lin, 2000);
- La température élevée de l'air en ville due à l'ICU vient déstabiliser l'atmosphère et peut générer des nuages convectifs (Li et al., 2020; Oke et al., 2017; Zhang et al., 2017);
- Une concentration plus importante d'aérosols au-dessus des villes due à la pollution est une source de noyaux de condensation (CCN) et influence le transfert radiatif entre la couche nuageuse et la surface. Ces effets sont résumés dans (Shepherd, 2013);
- Les systèmes tendent à bifurquer autour des villes (Bornstein & Lin, 2000) ou se séparer en petites cellules orageuses en amont des villes (Niyogi et al., 2011).

Ces processus sont complexes et difficiles à représenter adéquatement dans les modèles numériques. Liu & Niyogi (2019) rapportent des différences entre les études d'observation et de modélisation quant à l'impact des villes sur la précipitation, ces différences peuvent être expliquées par la représentation numérique de ces processus. Néanmoins, les expériences numériques sont de plus en plus utilisées afin d'approfondir notre compréhension des interactions entre les villes et l'atmosphère, puisque, ces expériences permettent d'isoler certains processus et donnent de l'information sur plusieurs variables.

Dans cette étude, des études de cas de prévision numérique du temps (NWP) sont effectuées dans la région de Montréal (Canada), qui est une région où d'importants ICU sont observés durant la période estivale. L'impact de la ville sur la température et sur le confort thermique est l'objet de plusieurs études (Oke & Maxwell, 1975, p. 197; Wang & Akbari, 2016), mais peu d'entre elles se sont penchées sur l'impact de Montréal sur la précipitation durant l'été. Étant située dans le fleuve Saint-Laurent, l'île de Montréal est souvent affectée par des inondations importantes. Au printemps, la fonte rapide de la neige conjointement aux précipitations plus importantes que la moyenne cause des inondations dans la région du Grand Montréal (Teufel et al., 2019). Durant l'été, par exemple, en juillet 1987, une série d'orages violents a traversé la ville de Montréal et a entraîné une crue soudaine qui a paralysé la ville. Cet évènement suivait une vague de chaleur extrême, qui a probablement intensifié les orages. Ce type d'évènement risque d'arriver plus souvent dans le futur puisque les zones urbaines ne cessent de grossir. De plus, outre l'environnement urbain, d'autres facteurs risquent d'intensifier les évènements extrêmes de précipitation. Par exemple, les températures plus élevées dues aux changements climatiques augmentent la capacité de l'atmosphère à contenir de l'eau (Trenberth, 2011). Une combinaison de ces deux facteurs risque d'affecter les populations urbaines dans le futur.

Les deux objectifs de cette étude sont de comprendre la manière dont l'environnement de Montréal influence la température et l'humidité locale pendant les périodes de forte chaleur et d'évaluer l'impact de la ville sur la précipitation suite à ces vagues de chaleur. Afin d'y arriver, deux évènements distincts de périodes de chaleur suivies de précipitation intense sont étudiés à l'aide d'un modèle numérique à très haute résolution. De plus, l'efficacité à réduire l'ICU de différents scénarios d'atténuation répliquant des stratégies de désign urbain est évaluée.

Le mémoire est structuré comme suit. Le chapitre 1 présente un article scientifique rédigé en anglais. La section 1.1 introduit le sujet et met en situation l'étude effectuée; la section 1.2 présente la méthodologie, les modèles utilisés et la configuration expérimentale; la section 1.3 présente les résultats des deux études de cas; la section 1.4 discute des résultats; et la section 1.5 résume et conclut des résultats principaux de cette étude. Puis, le mémoire se terminera par une conclusion générale rédigée en français.

CHAPITRE 1

EFFET DES SCÉNARIOS DE MITIGATION DE L'ÎLOT DE CHALEUR URBAIN SUR LA PRÉCIPITATION ET LA TEMPÉRATURE À MONTRÉAL, CANADA : DEUX ÉTUDES DE CAS

Ce chapitre comporte un article scientifique rédigé en quatre différentes sections. La section 1 correspond à la mise en contexte de l'étude scientifique. La section 2 présente la méthodologie expérimentale et les modèles utilisés. La section 3 de l'article présente les résultats des deux études de cas. La section 4 discute des résultats. Pour conclure, la section 5 résume et discute les résultats principaux de l'étude. Certains passages ont été modifiés par rapport à l'article scientifique accepté pour publicationafin de répondre aux besoins de ce mémoire.

EFFECT OF URBAN HEAT ISLAND MITIGATION STRATEGIES ON PRECIPITATION AND TEMPERATURE IN MONTREAL, CANADA: CASE STUDIES

Audrey Lauer[1]*, Francesco S.R. Pausata[1], Sylvie Leroyer[2], Daniel Argueso[3]

[1]Department of Earth and Atmospheric Sciences, University of Quebec in Montreal, Montreal, Quebec, Canada

[2]Meteorological Research Division, Environment and Climate Change Canada, Dorval, Quebec, Canada

[3]Physics Department, University of the Balearic Islands, Palma, Spain

Submitted to PLOS Climate on 2022-11-29 and accepted for publication on 2023-06-26

1.1 Introduction

Cities occupy a small fraction of the Earth's surface, yet over half of the world's population lives in urban areas, a number that is expected to significantly increase in the next decades (*World Urbanization Prospects*, 2019). Cities modify the local environment because they are built with materials and geometries that clearly differ from the natural landscape. Built structures have an impact on the local climate because they alter surface exchanges of heat, moisture, momentum, and radiation with the atmosphere. A complete understanding of these effects is crucial to identify and reduce the risks that urban dwellers are exposed to.

Initially observed and documented in the 1800s, urban areas are warmer relative to their rural surroundings (Mills, 2008). This phenomenon is referred to as the canopy urban hat island (UHI) and processes explaining the unique local climate of cities have been well documented (Oke, 1982; Stewart, 2011). Materials used in cities have low reflectance, are good thermal conductors and have greater heat storage capacity, so they are more efficient than the natural materials at absorbing atmospheric radiation fluxes and heat, which is then released at night mainly through sensible heat flux. Urban surfaces are mostly impervious, which alters the water budget by reducing infiltration and evaporation, and by increasing surface runoff. As a result, there is little water available for evaporative cooling and most turbulent heat exchanges are channelled through sensible heat fluxes. In addition, city landscapes are often less vegetated than rural areas, reducing evapotranspiration from plants and its effect on temperature. Urban geometry accentuates these effects by trapping energy because solar radiation is reflected multiple times by urban surfaces and thus the probability for it to be absorbed by the city fabric is larger (Oke et al., 2017). Urban areas reduce the wind, which enhances the heat trapping in the city (He et al., 2020; Oke et al., 2017). Anthropogenic heat sources (i.e. road traffic, industry, heating and air-conditioning) and atmospheric pollution also contribute to increasing the intensity of the urban heat island (Oke et al., 2017).

Urban planners tend to adopt many different strategies to reduce the strength of the UHI and its potential effects on the increasing urban population. Common mitigation strategies are, for example, adding green infrastructures such as green roofs, parks and trees (Berardi et al., 2020; Krayenhoff et al., 2020; Lee et al., 2016; J. Yang et al., 2016), and increasing the reflectivity of urban surfaces (Krayenhoff & Voogt, 2010; Taha et al., 1988; Taleghani & Berardi, 2018; J. Yang et al., 2016). Replacing urban surfaces with vegetation lowers air temperature due to increased evapotranspiration and less surface warming during the day.

Furthermore, low vegetation might enhance heat release at night since it often has a high sky-view factor. On the other hand, vegetation also adds water vapor to the air, potentially decreasing human comfort on local population. Studies show that in general heat stress is typically lowered when vegetation is added (Broadbent et al., 2018; Lee et al., 2016), which is beneficial to urban population. The type of vegetation (i.e. low or high vegetation) added and its placement inside the urban canyon can have a different effect on thermal comfort. For example, trees offer and are more effective than grass in improving comfort (Krayenhoff et al., 2020), since they offer shade. Increasing urban surface albedo decreases daytime air temperature due to higher reflection of solar radiation. Nighttime impacts of albedo change seem instead to be negligible (Taleghani & Berardi, 2018; F. Yang et al., 2011; J. Yang et al., 2016). For this mitigation strategy, the impact on human comfort can vary depending on the way it is assessed. Recent studies have shown that increasing the ground-level albedo may well decrease pedestrian comfort due to increased reflection (Erell et al., 2014; Herrmann & Matzarakis, 2012; Taleghani & Berardi, 2018). The effectiveness of these strategies is also greatly affected by the geographical location, size, and composition of the city. Also, the UHI intensity is typically greater at night than during the day, although the most important effect on human comfort are during daytime (Martilli et al., 2020). Therefore, the most effective heat mitigation measures are those that improve daytime comfort instead of the average UHI intensity.

In the last decade, it has also been shown that urban areas can have a sizeable impact on precipitation. Observational and modeling studies in mostly North American and Asian megacities reviewed by Liu & Niyogi (2019) show a rainfall enhancement of 16% over and 18% downwind of the city (20-50 km from the city center) (Liu & Niyogi, 2019). Our understanding on the urban processes that modify rainfall is still evolving because precipitation is influenced by many factors from large-scale synoptic systems to local cloud microphysics. The main mechanisms through which urban areas can influence precipitation are the following, in no particular order of importance:

- An increase in low-level convergence due to increased roughness of cities which impacts convection over the urban areas (Bornstein & Lin, 2000);
- Higher temperatures over cities due to the UHI tend to destabilize atmosphere, therefore create UHI-generated convective clouds (Li et al., 2020; Oke et al., 2017; Zhang et al., 2017);

- Enhanced concentration of atmospheric aerosols over cities due to pollution are sources of cloud condensation nuclei (CCN) and influence the radiative transfer between the cloud layer and the surface. These effects are summarized in (Shepherd, 2013);
- Storms tend to either bifurcate around cities (Bornstein & Lin, 2000) or split into small convective cells upwind from the city (Niyogi et al., 2011).

These processes are not always represented correctly in numerical studies, thus could explain the differences with observational studies reported in (Liu & Niyogi, 2019). Nevertheless, numerical experiments have become more and more important to understand interactions between the cities and the atmosphere as different urban processes can be isolated to disentangle their relative impact on local climate.

In this study, numerical weather prediction (NWP) case studies in the Montreal (Canada) region are explored. During summertime, important UHI both night and daytime can be observed in Montreal. While the impact of this city on temperature and heat stress has been previously investigated (Oke & Maxwell, 1975; Wang & Akbari, 2016), few studies have hitherto explored the impact of Montreal UHI on summertime precipitation. Located in the Saint-Laurence River, Montreal has been affected by significant flooding events. For example, springtime flooding in the Great Montreal region is typically linked to rainfall associated with extended thaw periods, hence leading to rapid melting of winter snowpack (Teufel et al., 2019). In July 1987, a series of strong thunderstorms that crossed the island in the afternoon generated significant downpours, which paralyzed the city. This event followed a significant heat wave over the region, which likely intensified the storm. Since previous studies have shown an enhancement of rainfall over urban areas and given that urbanized areas are growing, flooding events could be more likely to occur in the future (Madsen et al., 2014). Moreover, impervious surfaces in cities intensify surface runoff and reduces water infiltration, which increases the flooding frequency (Huong & Pathirana, 2013). Additional factors beyond the urban environment may produce an intensification of extreme events, for instance higher temperatures due to climate change increases the atmosphere's water-holding capacity (Trenberth, 2011). Studies have indeed shown a higher number of flooding events due to increasing urbanization and climate change (Huong & Pathirana, 2013; Kundzewicz et al., 2013; Miller & Hutchins, 2017), which urges cities to adapt.

The main objectives of this paper are, to understand how the urban environment of Montreal influences local temperature and human comfort during heat waves and to evaluate the impact of the city on rainfall following these heat waves. To achieve this, two heat events immediately followed by intense precipitation are studied using a high-resolution numerical model. Furthermore, different mitigation scenarios replicating urban design strategies are investigated to assess their effectiveness on improving comfort. The manuscript is divided as follows: section 2 presents the models used and the experimental design; section 3 shows the results from two different case studies; section 4 summarizes and discusses the key findings of this study.

1.2 Methodology

1.2.1 NWP models and system

The NWP experiments are conducted at a 250-m horizontal grid spacing. They are obtained through a nesting technique starting from the 2.5-km operational forecasts from Environment and Climate Change Canada (ECCC) High-Resolution Deterministic Prediction System (HRDPS) and dynamically downscaled to a 1-km and then 250-m resolution. The domains for the HRDPS and experiments at 1 km and 250 m centered on the city of Montreal are shown in the upper panel of Fig 1.

The atmospheric model used in this study is the Global Environmental Multiscale (GEM) model version 5.1 (Côté et al., 1998; Husain & Girard, 2017). GEM is a non-hydrostatic model on a staggered Arakawa-C horizontal grid and a staggered Charney-Phillips vertical grid. The configuration used in this work is based on a log-hydrostatic-pressure type terrain-following vertical coordinate.

In GEM, surface fluxes are calculated over 5 types of surfaces: natural land, water, glaciers, sea ice and urban. The surface processes over natural land including vegetation in urban areas are represented with the Interaction between Soil-Biosphere-Atmosphere (ISBA) scheme (Bélair et al., 2003; Noilhan & Planton, 1989). For built-up surfaces, the surface processes are represented with the Town Energy Balance (TEB) scheme (Lemonsu et al., 2009; Masson, 2000). The urban surface uses a canyon representation (Oke, 1981), which is a single road surrounded by buildings (walls and roofs) on each side. Interactions between surfaces such as shadowing and radiation trapping are considered by TEB and three distinct energy budgets are calculated – one for each surface. For water bodies, the surface temperature provided by the operational analysis is considered constant throughout the experiment, given water high heat capacity.

Ancillary data needed as input for TEB are computed directly on the model grid cell based on the methodology of Leroyer et al. (2022) and extended to the entire Canada including Montreal. The most important underlying vectorial dataset are Canvec and Circa-2000 (from Natural Resources Canada) NRCan databases and the Circa-2000 for vegetation and precise building heights and footprints for the downtown area (City of Montreal office). Morphological parameters including aerodynamical roughness are computed at the model grid resolution (Macdonald et al., 1998). Cloud and precipitation processes occurring at sub-grid scales are represented using four different schemes in GEM: a boundary layer clouds scheme, shallow and deep convection schemes and cloud microphysics. In this study, deep convection is considered explicitly resolved because the forecasts are done on a subkilometer grid and therefore the deep convection scheme is not activated. For boundary layer clouds and shallow convection, MoisTKE and Kuo Transient implicit schemes are activated. This configuration is further detailed in (Bélair et al., 2018). Finally, a two-moment version of the bulk microphysical scheme MY2 is used to represent the grid-scale processes (Milbrandt & Yau, 2005).

A similar setup has been used in many studies from ECCC (Bélair et al., 2018; Leroyer et al., 2022). This NWP system down to 250 m grid-spacing is experimental and was built similarly to the NWP system used for the Toronto metropolitan area (Canada) run daily for specific applications. Seasonal objective evaluation revealed a good representation of summertime afternoon convective precipitation (Lemonsu et al., 2009). At this scale, part of the turbulence is resolved and the thermal plumes in the mixed boundary-layer – eddies of the size of 1000-1500 m and more might be resolved (Honnert et al., 2020). The remaining sub-grid scale turbulent component, corresponding to smaller eddies, is computed through a vertical diffusion scheme for which a reduction of the maximum mixing length in neutral conditions from 200 m to 57 m has been applied (Mason & Brown, 1999).

1.2.2 Data for observations and analysis

Data from operational ECCC surface stations is used to evaluate the experiments. Hourly observations for surface variables are available for a few stations in the domain of interest (Fig 1.1, black dots). These stations are used to validate surface air temperature and humidity, as well as the timing and rainfall rate. More stations are available with daily observations (Fig 1.1, gray dots), which are used to compare total precipitation accumulations from our experiments. The complete list of stations with their description is available in the supporting materials (Table S1).

Due to precise representation of the elevation in the model and to moderate slopes in the region, elevation difference between model and in situ stations was found to be less than 10 m and is neglected in this study. In addition, 2-m temperature is computed above the road in the street directly and the reference level is not impacted by the large buildings in downtown.

Another dataset used for validation is the Canadian Precipitation Analysis (CaPA) dataset. The version used in this study is the High-Resolution Deterministic Precipitation Analysis (CaPA-HRDPA), which uses a background field from the HRDPS forecasts and observations from surface stations and radars (Fortin et al., 2018). 6-h accumulated precipitation at 2.5-km resolution is available for the two studied periods.

1.2.3 Experimental setup

1.2.3.1 Ensemble setup

In order to account for model internal variability, a 9-member ensemble is formed for each event as sketched in Fig A.1. Each member uses the same driving data from HRDPS forecasts (based on 12 to 24 hours lead-time forecasts), but has a different initialization date, each separated by 12 hours. This is a way for each member to have different initial conditions, and then to evolve in their own way, even with the same boundary conditions from the HRDPS forecasts. The last initialized member starts at least 12 h before the precipitation event to let the model spin-up. These first forecasted 12 h are not considered in our results analysis.

Initial surface conditions for ISBA are produced from the Canadian Land Data Assimilation System (CaLDAS) downscaled from 2.5 km to 1 km and 250 m and for water bodies from ECCC's analysis. Temperature of the urban surfaces in TEB in contact with the atmosphere is considered the same as the surrounding air temperature at the time of the initialization (surface layer for roads and walls, and first atmospheric level for roofs). Temperature in the deepest layer of road is assumed similar to the soil temperature from ISBA. In addition, a 12-hours spin-up time is considered for the surface temperatures to adjust.

1.2.3.2 Sensitivity experiments

Four sensitivity experiments are carried out on both the 250-m and 1-km grid for each ensemble member: a control simulation (CTL) using the default land use (as depicted in Fig 1.1), an experiment without any urban areas (NOURB), a simulation in which the albedo of the urban surfaces is increased (ALB) and another one in which urban vegetation is enhanced (VEG). In the CTL simulation, the urban surface is

represented by using a database of rasterized maps of detailed urban and natural classes at a 5-m resolution, following the method used in Leroyer et al. (2022) for Toronto. In the NOURB experiment, every urban surface (roads and roofs) is replaced by low vegetation and the TEB scheme is deactivated. In the ALB simulation, the albedo of roads, walls and roofs is modified over 85% of the grid points on the island of Montreal. Road, roof and building wall albedo are increased from 0.20, 0.15 and 0.25 to 0.45, 0.65 and 0.60 respectively. Other city properties (i.e. geometry, composition and materials) are not modified in the ALB experiment.

In VEG, we replace half of the roads on each grid point with low vegetation if the original road fraction is between 0.2 and 0.5. An important thing to note on the operation of the TEB scheme is its separation of urban land use from natural cover. Both are considered completely separated – TEB will calculate variables (i.e. air temperature, humidity and winds) inside the canyon, the ISBA scheme will calculate these variables over vegetation, and weighted average is done for the whole grid point afterwards. To keep the city's geometry fixed, the building aspect ratio is kept the same. In other words, the surface description used by TEB is similar in both VEG and CTL, but the weight attributed to the ISBA scheme's results at the time of the aggregation will be larger.

1.2.4 Description of the events

This study focuses on two distinct events where surface air temperature values above 30°C in Montreal were followed by remarkable rainfall.

The first studied period is in July 2018 (SYNOPTIC, Fig 1.2), when hot days (with temperature values progressively increased up to about 32.5°C) were followed by a significant rainfall event over the Montreal region associated with a large-scale synoptic system crossing the Montreal Island from the southwest. The radar images available in the Supplementary Materials (S2 Fig) show the propagation of the system. The event occurred during late night/early morning and brought intense precipitation between 0400 and 0800 local time on the 17th of July 2018 with hourly rainfall amounts reaching about 10-15 mm. A complete analysis of this event will be done in the following sections.

The second studied period is in July 2019 (SQUALL), where a series of hot days with temperature reaching up to 30°C was followed by intense precipitation in the Montreal region. A squall line travelled from the northwest and brought heavy rain and thunderstorms in the region during the late afternoon of the 11th

of July 2019 (Fig 1.3). The radar images available in the Supplementary Materials (S3 Fig) show the propagation of the squall line near Montreal. The line is well defined while approaching Montreal, when it seems to split right before crossing the city and then merges over the southeast part of the city. These systems are typically very unstable and can be further destabilized as cold and humid air travels through hot and dry air over urban areas.

1.3 Results

This section is divided in 3 parts. In the first part (Sect. 1.3.1) we validate the model performance in representing the urban processes and the rainfall events against observations. In Section 1.3.2 we look at the effects on surface air temperature and humidity of each mitigation scenarios and finally in Section 1.3.3 we investigate the impacts of NOURB experiment on rainfall relative to the CTL case.

1.3.1 Control experiment (CTL) versus observations

1.3.1.1 Surface variables in the CTL experiment

Results for two stations for the SYNOPTIC event are analyzed in this section: McTavish station (WTA) which is in a dense urban area in downtown Montreal, and St-Hubert Airport station (YHU) which is in a suburban area east of Montreal (Fig 1.1).

The model captures well the surface air temperature diurnal cycle during the days prior to the rain event at different locations in the area, especially in the 250-m experiments. First, we look at the 250-m resolution results (Fig 1.4a and 1.5a) for the SYNOPTIC event. Daily maximum temperatures at the urban station (McTavish, Fig 1.4a) for the 3 days leading to the precipitation event are higher by 1-2°C in the CTL experiment than the observation. Such discrepancy is likely due to the fact that measurements are done at a single point, usually over low grass or bare soil (World Meteorological Organization (WMO), 2018), whereas the model computes an average over all urban surfaces in a 250-m radius. Hence, in the model the output, temperatures also include temperatures over urban surfaces, which are warmer than bare soil and vegetation during the day. At the suburban station (St-Hubert Airport, Fig 1.5a), maximum temperature is similar in the CTL experiment and the observations. The station is located outside the urban area (Fig 1.1), where the land use is more uniform (i.e. large fields and roads), thus the conditions experienced by the sensor are more representative of the model grid point average. In the 1-km resolution CTL experiments (Fig 1.4b and 1.5b), the model is also able to capture well the air surface temperature,

although the differences in the maxima between the model and the observations are larger than in the 250-m experiments.

For the SYNOPTIC event at the 250-m resolution, at both stations, the temperature from July 14th to the early hours of July 15th of the CTL experiment differs quite substantially from observations (Fig 1.5a and 1.6a). The forecasted daytime surface air temperatures are around 2°C higher and nighttime temperatures around 1-2°C cooler than observed temperatures. This indicates a somewhat incorrect model representation of some processes, possibly related to cloud cover or inexact representation of the boundary layer. On the other hand, for the two days leading to the event (July 15th and July 16th) the model correctly captures the surface air temperature diurnal cycle.

Regarding surface dew-point temperature, the results from CTL tend to agree with the available observations but present slight differences (Fig 1.4c, Fig 1.5c). In particular, the dew point model behaviour on July 15 and 16th seems delayed by a few hours compared to observations. No delay is simulated in the air temperature, suggesting that the discrepancy in simulating the dew point could be due to a delay in the large-scale moisture advection. During the precipitation events (on July 17th), modelled surface dew point temperature agrees well with observations both on timing and value.

The SQUALL event shows a similar behavior (Fig 1.6 and 1.7). Air temperature in CTL follows quite closely the observations, although maximum daily temperatures are overestimated (as explained above). During the morning leading to the precipitation event, the model shows a rise of temperature to up to 30°C a few hours before the observations, which we can attribute to clouds that are not simulated in CTL. As for dew point temperature, the model presents slight differences with the observations throughout the period. As for the SYNOPTIC event, a delay in the rise of dew point on the day of the event is present in CTL.

Results for other stations are available in the supporting materials for SYNOPTIC (Fig. B.2, B.3, B.4). The 250-m resolution experiments follow more closely observations than the 1-km experiments. Daily surface air temperature maximas and minimas are better represented at the higher resolution for the downtown and suburban stations. In both cases, the dewpoint presents slight differences with observations. The bias and standard deviation, indicated on the top left of each figure, is generally better in the 250-m resolution experiments for all stations, except the Granby station (MGB) (Fig. B.4), where the model at 250-m resolution strongly overestimates the daily maximum temperature. This needs to be investigated further, as the model might misrepresent physical processes in that region. Overall, the ability of the model to

represent adequately air temperature and dew point indicates an overall good performance in capturing the surface processes. The 250-m resolution experiment will be used as the reference in the following sections. Precipitation in the CTL experiment

The SYNOPTIC event is a large-scale system that crosses the Montreal Island and travels following the St-Laurent River from the southwest to the northeast. Two accumulation maxima are present in the CaPA analysis on both shores of the St-Laurence River (Fig 1.8i). The first maximum on the southeast shore of the river is well reproduced in the CTL experiment, with similar intensities and shape. The second maximum over the island of Montreal and on the northwest shore of the river is less intense in the model relative to the CaPA analysis. The model strongly underestimates this maximum, as if it was supressed completely, with less than 20 mm in the 24-hour accumulated precipitation on most of the grid points on the northwestern shore. On the other hand, a strong maximum in the southwest of the island is shown in the CTL results, which is absent in the CaPA analysis.

Hourly accumulations are available at a few stations in the area providing more details on the evolution of the rainfall event (Fig 1.8). Considering the system travelling from the southwest to the northeast, we accordingly choose four stations to investigate hourly rainfall intensities (see stations location in Fig 1.1) as follows: (a) a station upwind southwest of downtown (Sainte-Anne de Bellevue, WYQ), (b) a station in the downtown area (McTavish, WTA), (c) a station east of downtown (St-Hubert Airport, YHU) on the southeast shore of the river, and (d) a station downwind north of downtown (L'Assomption, WEW). Precipitation is simulated in the CTL experiment at around the same time as the observations, but intensities differ.

Both the 24-h accumulations (Fig 1.8j) and the hourly precipitation in the CTL experiment seem to indicate the system is slightly blocked by the city and bifurcates on the south shore of the St-Laurent river only. Considering the split of the system on each shore of the river in the observation (Fig 1.8i), the cell on the southeast shore is well represented in the model as shown at station YHU (Fig 1.8c), but the part passing over the city (defined by the path of stations WVQ, WTA and WEW) seemed blocked before crossing. The model simulates strong accumulations upwind (Fig 1.8a), consistent with observations, and very little rainfall over the city downtown (Fig 1.8b) and downwind (Fig 1.8d), underestimating accumulation in comparison to observations. The 1-km results (Fig 1.9 e-h) results show the same trends as those from the

250-m resolution experiments (Fig 1.9 a-d). Intensities differ slightly between both resolutions, and the timing at the studied stations is similar.

The SQUALL event is a squall line that crosses perpendicularly the St-Laurence River and the island of Montreal during the afternoon from northwest to southeast (Fig 1.9i). The radar shows the squall line split before crossing the city (C.1 Fig), which can also be noticed in the CaPA analysis, where there are two poles of intense precipitation located on the northern and southwestern parts of the island, and lower intensity in the center (Fig 1.9i). Both poles seem to regroup over and downwind from the city to form a weaker squall line with the same propagation direction. The model simulates the squall line, with the same propagation direction and timing as the observed one, although convection over the city seem completely supressed (Fig 1.10). It splits into two smaller cells right before crossing the island, but contrary to the radar observations, both cells do not merge downwind of the city. This causes the dissipation of the squall line and therefore there is barely any precipitation downwind from the city (east and southeast of the Montreal island).

We choose four stations according to the propagation direction of the system to investigate hourly rainfall intensities in the 250-m experiments (Fig 1.9 a-d) as follows: (a) a station upwind (L'Assomption, WEW), (b) a station in the downtown area (McTavish, WTA), (c) a station southwest of downtown (Pierre-Elliott-Trudeau Airport, YUL), and (d) a station downwind east of downtown (St-Hubert Airport, YHU). At the stations upwind (WEW), downtown (WTA) and downwind (YHU), hourly observations show an intense peak of precipitation in the first two hours (20-30 mm) followed by a trail of less than 10 mm for the next two hours. The same signal is observed at the station YUL, but with lower hourly accumulations (less than 10 mm during the first hour). The model is consistent with observations upwind (Fig 1.9a), with about 30 mm accumulated rainfall in the first two hours, followed by traces of precipitation in the next two hours. As for the other three stations (Fig 1.9b,c,d), the model rather simulates a 4-hour period of constant rainfall (less than 5 mm/h), which indicates a dissipation of the squall line over the island of Montreal.

In both cases, the model seems to overestimate the blocking of the precipitation system before the city. In the SYNOPTIC event, accumulated precipitation indicated a blockage upwind and a possible bifurcation south of the city. In the SQUALL event, the squall line seems to dissipate before crossing the river. In following sections, we will investigate whether this behavior is due to the presence of the city in the CTL experiment.

1.3.2 Effect on surface air temperature and humidity of mitigation scenarios

In this section, we investigate how the urban land-use/land-cover influences the surface air temperature, humidity and heat index, by either completely removing the urban area or by using heat mitigation scenarios. In the following subsections, only the member average is presented and analyzed. The impact of these land-use changes is shown in two types of figures. First, we look and the spatial average and variability over the island of Montreal (Fig 1.11 and C.3) for the member average. The black line is the spatial average on the island, and the grey zone represents the 5^{th} to 9^{th} percentile of spatial variability. Second, we look at maps of the differences from the member average (Fig 1.12, B.5, B.6 and C.4), since it gives information about that previously analyzed spatial variability.

1.3.2.1 NOURB versus CTL – surface

To quantify the impact of the city, we replace urban areas with vegetation in the NOURB experiment as described in section 1.2.3.2.

As expected, replacing all urban areas by vegetation significantly reduces surface air temperature (Fig 1.11a), with maximum differences up to 4-5°C at night. Thermal properties of urban surfaces cause them to be more efficient than rural areas in storing heat, which is then released into the atmosphere during the night. This heat release increases the surface air temperature over urban surfaces, which explains such large temperature anomaly when they are removed in the NOURB experiment. Dew point, on the other hand, is up to 2-4°C higher in the NOURB run than in the CTL run (Fig 1.11b), reaching maximum differences during the afternoon and at night. Such an increase is due to added water vapor from evapotranspiration.

The comfort felt by the city's inhabitants depends mostly on air temperature and humidity. A way to define this comfort is by calculating a heat index. The U.S. National Weather Service (NWS) algorithm is used in this study (Anderson et al., 2013). According to this algorithm, we find that heat index is decreased quite substantially in the NOURB experiment compared to the CTL experiment (Fig 1.11c). At night, there is an average decrease of heat index of 2-4°C, with local peaks of up to 6°C in the downtown area. During the day, the decrease of heat index is less noticeable, and it is around 1°C.

The surface landscape and possible wind advection strongly determine the spatial pattern of the heat index, temperature, and humidity anomalies (Fig 1.12). Denser urban areas show a more substantial temperature and moisture differences than rural areas, as expected. A dispersion plot of the temperature

differences between NOURB and CTL versus the urban fraction of the gridpoint (Fig 1.13) shows this trend. Higher urban fractions (dense areas) have a larger temperature difference than gridpoints with a low urban fraction. Although these modifications are local, the hot and dry air is advected outside the city according to the wind's direction.

These results show how much the presence of a city like Montreal can modify the environmental properties of the city and surrounding areas, making it warmer and drier than the rural regions. The results for the SQUALL event are available in the supporting materials (Fig C.3 and C.4). Intensities of differences between the NOURB and CTL are slightly lower for the SQUALL event than the SYNOPTIC event. Maximum daily temperatures during the SQUALL event (30°C) are lower than during the SYNOPTIC event (32°C), which indicates proportionality between the strength of the UHI and high temperatures. Our results also show the same diurnal pattern in both the 2018 and 2019 events, with the largest differences in heat index at night. Both events show similar advection patterns, however the signal is less clear in the SQUALL event rather than during the SYNOPTIC event due to the surface wind that changes direction the day prior to the precipitation event.

1.3.2.2 ALB versus CTL - surface

In the ALB experiment only surface reflectivity is increased – the city's geometry, composition and materials are kept as in the CTL simulation, therefore thermal properties are not modified.

Surface air temperature is decreased throughout the whole day in the ALB experiment compared to the CTL experiment (Fig 1.11d), but to a lesser degree than in NOURB. As expected, this decrease is most important during the afternoon when the solar radiation is at its strongest. The higher albedo reflects more shortwave radiation in the ALB experiment; therefore, the brighter urban surface will warm less than the darker CTL surface. On the other hand, nighttime air temperatures in the ALB experiment are only slightly lower than in CTL (less than 0.5°C). This is expected since emissivity and thermal properties of materials were not modified. The white and dark surfaces both release heat at night at similar rates; therefore, the nighttime UHI is not significantly affected by changes in albedo. The slight decrease in temperature can be associated with the fact that less heat is stored in the surfaces during the day.

The change in albedo slightly affects moisture (Fig 1.11e). Dew point is increased up to 1°C during the afternoon in the ABL experiment compared to the CTL. Overall, the heat stress is lowered by the increased albedo (Fig 1.11f), which is in turn beneficial for the population living in the city.

1.3.2.3 VEG versus CTL – surface

In the VEG experiment, parts of the roads are replaced by low vegetation and the city's geometry is not modified compared to the CTL simulation. Considering the configuration used in the experiment, the weight attributed to the natural land cover fraction relative to the CTL will be more important in the VEG experiment; however, the natural land cover fraction is much less dominant in the VEG than in the NOURB experiment.

Vegetation has different properties than asphalt and cement roads, in particularly albedo, emissivity, soil moisture evolution through the day and presence of evapotranspiration. Therefore, air is cooler and moister over vegetation than over urban cover. Since the weight attributed to vegetation is larger in the VEG experiment than in the CTL, the overall results show a slight decrease in 2-m air temperature and a slight increase of dew point (Fig 1.11g,h). Some single grid points show the opposite behavior, especially in less dense areas, where the VEG experiment showed higher temperatures and lower dew point than the CTL experiment (Fig B.6a,b,c). As those anomalies are isolated and located outside of the main urban core, the benefits of the scenario are still relevant.

These factors create a mixed effect on heat stress (Fig 1.11i), with areas that show a slight increase of comfort and others a slight decrease; in particular, an overall increase of comfort is simulated in dense urban areas (Fig B.6).

1.3.3 Effect on precipitation of mitigation scenarios

The results presented in section 1.3.2 indicate the clear impact of the urban land use on temperature and humidity at the surface. In this section, we investigate whether this modification of the surface layer properties (NOURB) can possibly affect rainfall.

1.3.3.1 SYNOPTIC event

In terms of the effect of Montreal urban area on rainfall during SYNOPTIC event, when the system passes through Montreal at night, our model experiment does not show any significant impact in terms of

cumulative amount during 24 hours (Fig 1.14). To asses the significance of the precipitation differences, a Student's t-test considering a p-value of under 0.1 is computed at each grip point. The results of this statistical test is overlayed to the precipitation difference map (black dots). Therefore, most small differences between NOURB and CTL are just random noise from the ensemble average. Some significant differences are present on the outside of the Montreal, which are hard to explain in the context of our numerical experiments. As mentioned in section 1.3.1.2, the CTL experiment shows less precipitation than observations over the city and downwind of the city, which we initially surmised to be related to the city's parametrisation in the model. However, replacing the urban surfaces and decreasing the roughness in the NOURB run does not seem to change the precipitation pattern. Therefore, the decreased rainfall over the city area in the CTL experiment cannot be due to the presence of built-up surfaces.

In addition, the surface instability caused by the UHI seems negligible in this case, as the rainfall event is part of a well-organized synoptic scale system. A vertical sounding of the modelled atmosphere in the CTL experiment at the start of the event shows very little convective available potential energy (CAPE) and a large zone of convective inhibition (CIN) at the surface (Fig 1.16a), which indicates low atmospheric instability in the region. Modifying the land properties is expected to affect only the lower atmospheric levels, which is visible in the skew-T (Fig 1.16b). Hot and dry surface air in the CTL run generates a smaller surface CIN region compared to the NOURB run, but this reduction of CIN is not sufficient to provide a detectable impact on the system.

1.3.3.2 SQUALL event

As opposed to the SYNOPTIC event, the SQUALL event is characterized by high instability. The front edge of the squall line is typically very unstable, with strong updrafts of moist air and the system travels over the city in the afternoon, when instability is at its maximum. Our results show a displacement of heavy rainfall towards the city in the NOURB simulation (Fig 1.15) compared to the CTL experiment. Analysis of the composite reflectivity calculated by the model for the NOURB and CTL experiment shows no visible differences in timing and propagation of the squall line (Fig 1.10; the results at 1-km resolution are shown in order to see a larger portion of the squall line). In both cases, the system arrives at the city at 19:00 local time with strong intensity. The intensity of the squall line dissipates by splitting in small cells as it travels over Montreal (Fig C.1). Accumulated rainfall differences between the NOURB and the CTL experiment show a signal at approximately the same location as the dissipation (over the city). There is a translation of accumulated rainfall of 10 mm more towards the island of Montreal in the NOURB experiment. In both

cases, the squall line loses a lot on intensity downwind of the city, but it continues with the same propagation direction. This indicates that the presence of the city seems to affect the system on the upwind side of the island only.

The atmosphere is quite stable right before the passage of the squall line (Fig 1.17). As the system passes over the island of Montreal, a large area of CAPE is present in the vertical sounding. The CTL experiment (Fig 1.17c,e) shows a significantly larger CAPE area than the NOURB experiment (Fig 1.17d,f) which indicates that the presence of the city has more potential of enhancing convection. In our case, the squall line splits over the island of Montreal in both the CTL and NOURB experiments, which might explain why there is no significant effect on precipitation.

1.4 Discussion

Using a 250-m grid spacing for this type of study is interesting for many reasons. First, the surface heterogeneity is represented with very high accuracy and precision, therefore local processes of the urban heat island can be parametrized and resolved. A study from Leroyer et al. (2022) with a similar setup at 250-m horizontal resolution has proven better results than the 2.5-km operational analysis for 2-m temperature, dewpoint, winds and precipitation in summertime in Toronto (Leroyer et al., 2022). Precipitation patterns showed more details and have the potential to represent processes that cannot be resolved with the 2.5-km resolution (Leroyer et al., 2022). However, NWP experiments at hectometric horizontal resolution are still experimental and further studies are necessary to strengthen their applicability.

1.4.1 Surface variables

The results presented in the study for 2-m temperature, dew point and thermal comfort agree with the existing literature. The NOURB experiment, in which all urban areas are replaced by low vegetation, highlights the intensity of the urban-induced modifications to local microclimate. The 2-m air temperature is greatly decreased especially at night, where differences with the CTL experiment reach 4-5°C. The simulated anomalies are consistent with the difference in temperature between the urban station (McTavish, WTA) and the rural stations of Mirabel (YMX) to the west and Saint Hubert (YHU) to the east. Available observations show about the same maximum daily temperature between the urban station and the rural stations, but a 5°C difference in minimum temperature. This decrease in temperature is well documented and the urban processes are well understood (Oke et al., 2017). The added vegetation also

has the effect of adding moisture in the air due to evapotranspiration, but, overall, the thermal comfort is improved in the NOURB experiment on average around 2-4°C, and around 1°C during the day on average. However, a notable spatial variability in the heat index anomalies is simulated over the island of Montreal, with larger differences over dense urban areas (4-6°C) and negligible effects over existing large parks and low urban density areas. Therefore, mitigating the effect of the UHI has the potential to lead to a remarkable increase in human comfort for the population living in the city.

The spatial variability is visible in the maps of differences between the NOURB and CTL experiment (Fig 1.12) and the scatter plots of the differences (Fig 1.13). Although the differences in temperature between both experiments is more important when the urban fraction is higher (negative trendline, the dispersion within the individual gridpoints is large. This can be attributed to different factors, for example the road and building partitioning, or that the neighboring gridpoints influence each other and surface wind advect the air towards other areas.

In our study, we perform two mitigation scenarios, 1) increasing the urban surface's albedo (ALB) and 2) adding low vegetation at the street level (VEG). The increased albedo experiment shows a reduction of surface air temperature peaking during the afternoon, while nighttime temperature modification is negligible. According to literature, peak decrease of temperature due happens when sun radiation is maximal. At night, the air temperature is expected to be decreased in the ALB experiment compared to CTL, since there is less heating of the surface during the day (Redon et al., 2017). Our results show this behavior, although the difference in temperature reaches almost zero as the end of the night. Our results show a slight increase of moisture during daytime in the ALB experiment, possibly due to an indirect effect on condensation. Overall, this strategy increases thermal comfort by 0.5-1°C during the day. There are many ways to calculate the thermal comfort. In this study, the NWS heat index is used, which takes into consideration temperature and humidity. Other comfort indices also consider radiative exchanges at the street-level and winds, and studies have shown that increasing the ground-level albedo tend to decrease pedestrian comfort due to increased reflection (Erell et al., 2014; Herrmann & Matzarakis, 2012; Taleghani & Berardi, 2018). No detailed analysis of the comfort was conducted as it is outside the scope of this study, therefore results on comfort changes for the ALB experiment must be interpreted carefully and are more representative of no-ground level albedo change. Further studies on the impact of mitigation scenarios on other comfort indices are necessary.

Adding low vegetation at the street level (VEG) in our numerical experiment shows a marginal and mixed impact on improving thermal comfort with slight reduced temperature and increased humidity. However, in dense urban areas, our results do show a decrease in temperature large enough to improve comfort. Adding trees instead of low vegetation would certainly have a more positive impact on thermal comfort since they interact directly with radiation by shading the surface (Oke et al., 2017). This scenario was not considered, as such effect is not represented in our model. Investigation with other urban schemes in which the effect of trees is accounted for would provide better insights on mitigation strategies(Redon et al., 2017). The results from the mitigation scenarios presented in this paper are in agreement with a similar study done for Montreal's local authorities (Leroyer et al., 2019) in which the effect of multiple mitigation scenarios is analyzed. Furthermore, Leroyer et al. showed that the small reduction of air temperature (< 0.5°C) associate with adding street-level vegetation could be greatly increased with forced soil irrigation (around 1°C). Hence, a combination of increased albedo and vegetation, would be greatly beneficial for the population living in dense urban areas.

1.4.2 Precipitation

For the SYNOPTIC event, in which an organized frontal system crossed the city at night, the impact on precipitation from the urban land use is not detected in our numerical experiments. The main reason is probably related to the fact that the UHI induced modification of the air mass above the city is not large enough to affect a large-scale organized system. These system's trajectories and intensity are defined by synoptic factors and a small perturbation at the surface has likely no impact. Furthermore, even if the signal of the UHI is strongest at night, the atmosphere is typically very stable, as compared to during the day, where the surface is very hot and generates substantial vertical instability. Nevertheless, Li et al. (22) have shown that in some cases, the UHI impacts on surface variables have a significant effect on atmospheric stability and hence, can enhance rainfall.

For this reason, we investigate another event in 2019 (SQUALL), characterized by large instability as a squall line develops in the afternoon and crosses Montreal from the northwest. In this case, the city seems to slightly affect the system. Results revealed more rainfall over the city in the CTL experiment compared to the NOURB case. The different spatial pattern of accumulated precipitation from the CTL and NOURB experiment shows a signal that indicates a possible impact from the land use: when the city is present the front seemed to be blocked before the island of Montreal before dissolving. The analysis of the vertical profile over the downtown area showed a large CAPE area at the time of the storm, which is significantly

larger in the CTL experiment than NOURB. This indicates that the UHI can notably increase convection and instability, and therefore intensify the storm. However, in our experiment the squall line splits and weakens before passing over the city, which may explain why there is no significant differences on precipitation downwind of the city. Nevertheless, our results highlight how the presence of a large urban area can affect the vertical stability of the atmosphere, especially during periods of high instability.

Such impact on precipitation supports the finding of the above-mentioned study by Li et al. (22), suggesting an impact on rainfall of the UHI. However, our study indicates that conclusions on modification of precipitation due to urban land-use from isolated case studies have to be interpreted carefully as rainfall is highly variable and can be associated with different meteorological conditions. Therefore, other rainfall events, such as more localized events spurred by the instability created by the presence of the city itself should be considered to gain a more robust understanding of the city impacts on precipitation. Furthermore, a model intercomparison and further investigation on the model configuration and the schemes used for the representation of physical processes at the surface and in the boundary layer could help shedding light on model inaccuracy and misrepresentation of the rainfall systems.

A small number of ensemble members was used to reduce the effects of the model internal variability. Precipitation is a hard variable to modelize accurately – many different factors will influence the precipitation outputs. Since our numerical setup of the CTL run was able to modelize both systems with good accuracy and timing, our results can give insight into the effect of the city on precipitation.

1.5 Conclusion

The objective of this study is to determine potential effects of the city of Montreal and the impact of different urban development strategies on the local climate. At present, studies have investigated the UHI in Montreal (Oke & Maxwell, 1975; Wang & Akbari, 2016) and the possible impact of mitigation scenarios (Leroyer et al., 2019); however, little is known on the UHI impact on summer rainfall. Numerical experiments with a subkilometer (250 m) Numerical Weather Prediction System using GEM as atmospheric model and TEB as surface scheme are performed, following recent configurations used for urban studies at ECCC (Leroyer et al., 2022).

Local surface climate is in general well represented by our numerical model. Overall, air temperature and dew-point temperature followed accurately the observations available for the studied periods with some

minor discrepancies. As for precipitation, the model was able to simulate the rainfall event for both the SYNOPTIC and SQUALL events, although presented differences with the observations. In both cases, accumulated precipitation was lower over and downwind of the city, suggesting a possible blockage of the systems by the city. This conclusion has to be interpreted carefully, as low number of ensemble members and case studies were used in this study.

Finally, Montreal has a particular geographical setting since it is an island in the St-Laurent River valley, which influences winds and precipitation (Carrera et al., 2009; Dookhie, 2011). It is thought that storms have the tendency to bifurcate or split around Montreal. This phenomenon has not been yet studied, but it has been surmised that the river could modify low-level divergence and therefore protect the island from strong storms (Ouellette-Vézina, 2022). The 2018 event did not show this behavior, but the model simulated a bifurcation of the system in all experiments. Observations as well as the experiments of the 2019 event showed a split of the squall line, although the model misses the merge of the system over the city. It may well be that our model overestimates the processes that influence the bifurcation and split. Additional studies of model sensitivity to the river properties (temperature and presence) and for other heavy rain events are necessary to shed light on the role of Montreal island in bifurcating or splitting storms.

FIGURES

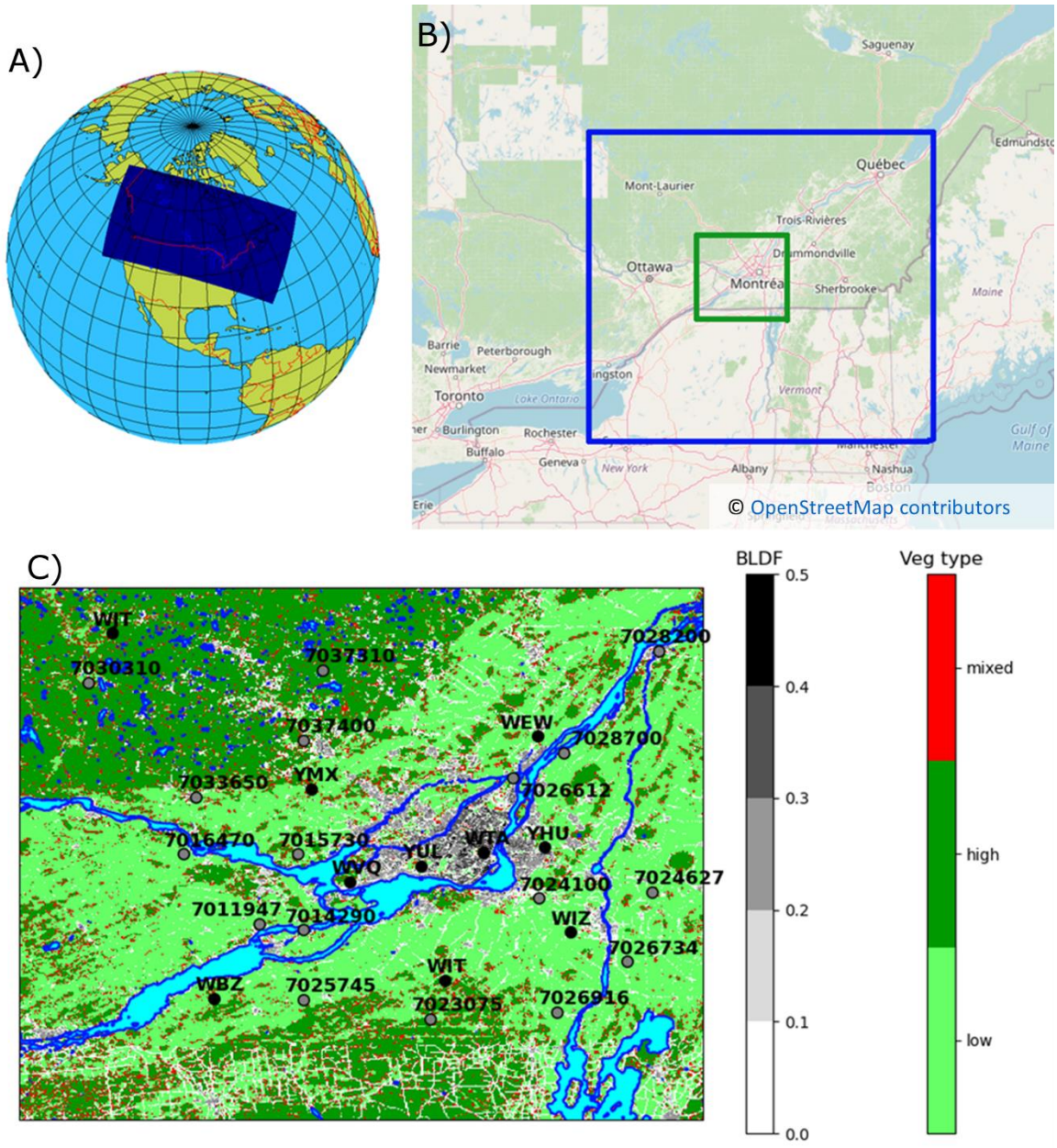

Figure 1.1. **Geographical locations of model domains and weather stations.** a) The HDRPS (2.5 km) domain over North America used to drive our model simulations, b) The high-resolution domains at 1km (blue rectangle) and 250m (green rectangle) and c) details of land use on the 250 m grid. The grayscale shows the building fraction, with main roads added in white. The green-red scale shows the main type of vegetation at the grid point. Weather stations are shown (in black: hourly observations; in grey: daily observations) with their corresponding national identification (refer to table in the supporting materials for details of stations)

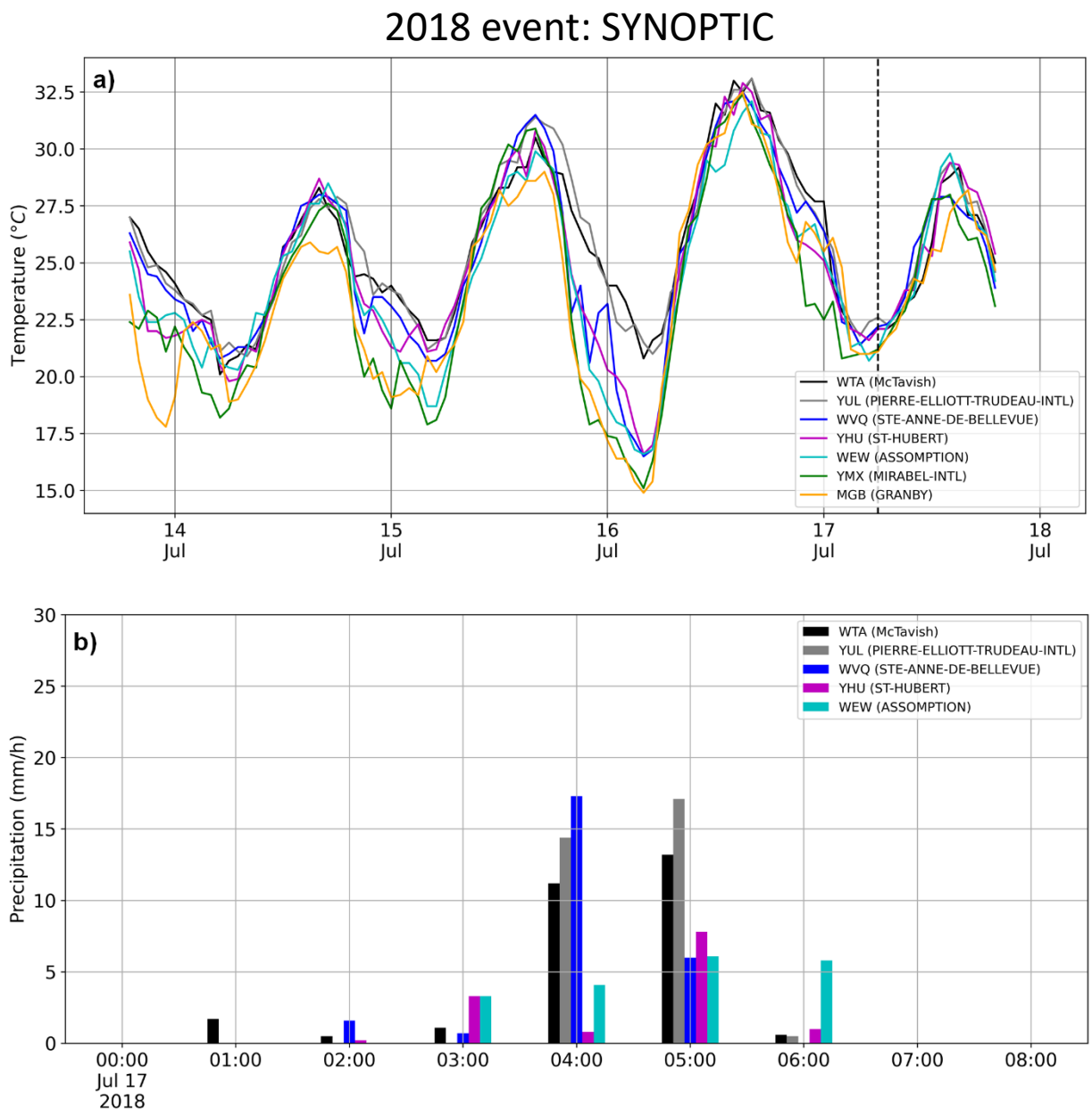

Figure 1.2. **Observed temperature and precipitation for the SYNOPTIC event.** Observed hourly a) surface temperature and b) precipitation accumulation at different stations. Precipitation data is missing for Mirabel-Intl and Ste-Anne de Bellevue stations during that period.

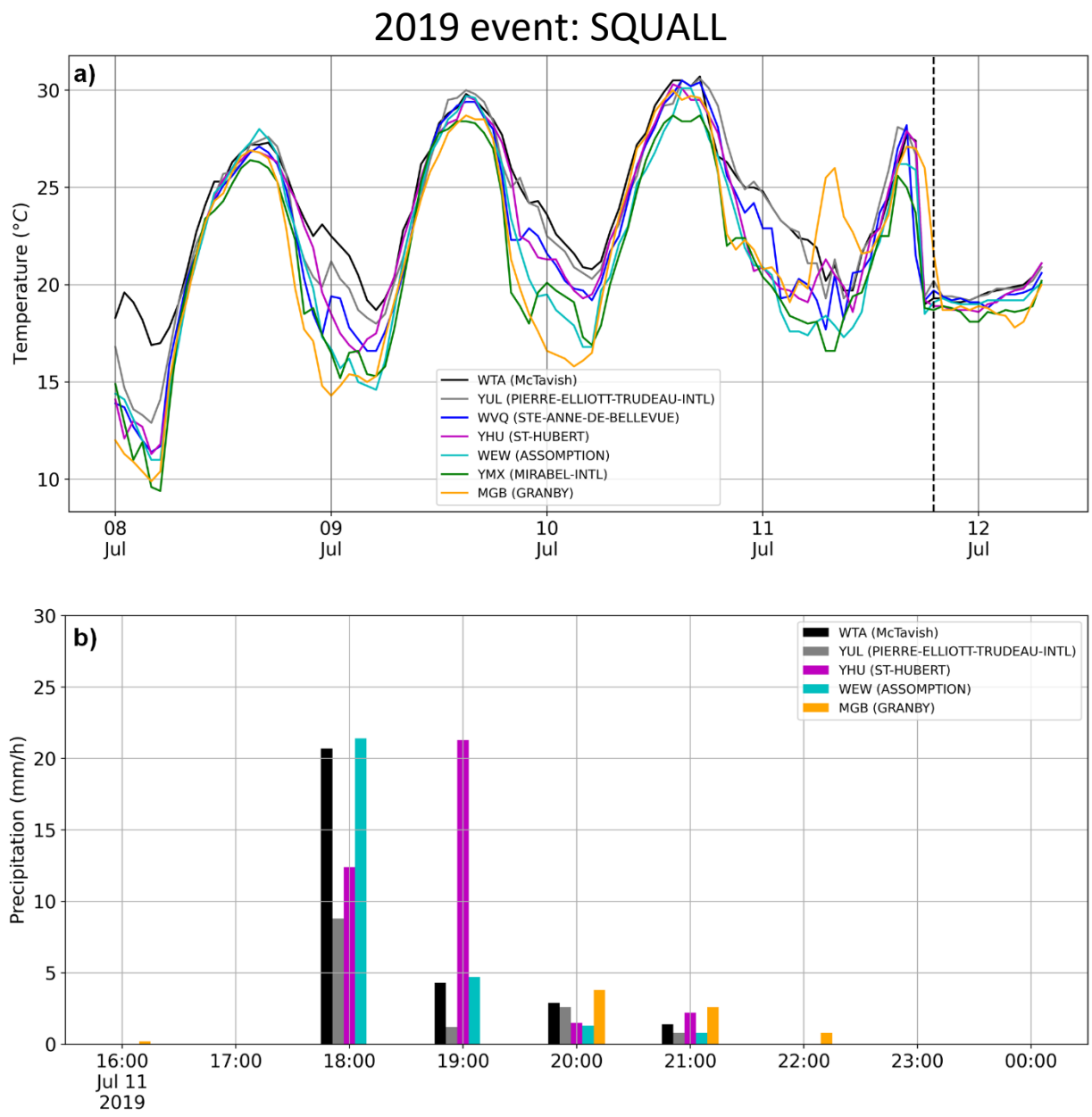

Figure 1.3. **Observed temperature and precipitation for the SQUALL event**. Same as Fig 1.3 for SQUALL case study.

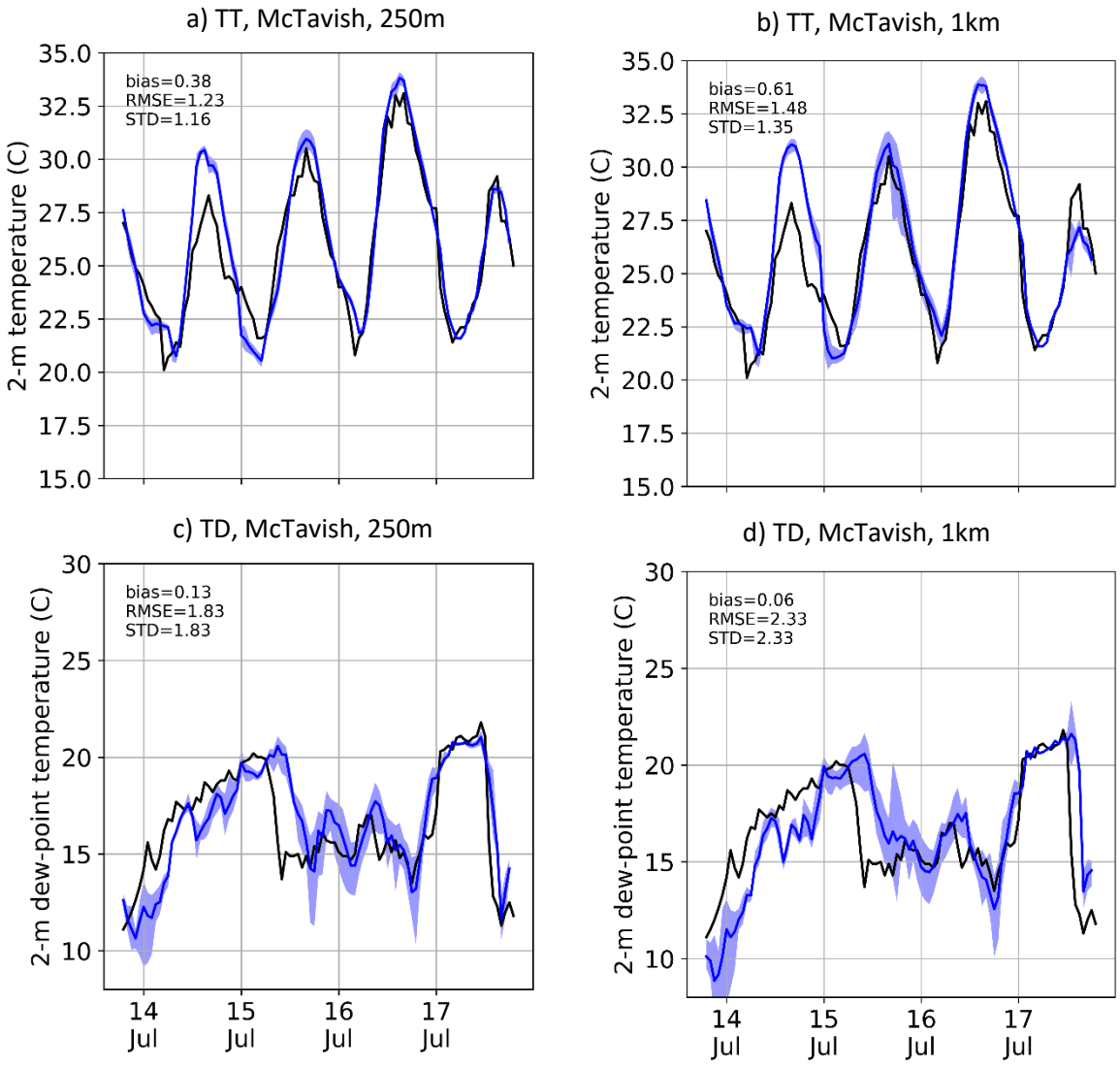

Figure 1.4. **Timeseries of observed and simulated surface variables at McTavish for the SYNOPTIC event.** Observed (black) and simulated (blue) surface air temperature (a,b) and dew point temperature (c,d) at station McTavish (WTA) for the SYNOPTIC event. Left panel are the results of the 250m resolution experiments (a,c) and right panel are the 1km resolution experiments (b,d). The blue shading shows the ensemble spread (5^{th} to 95^{th} percentiles).

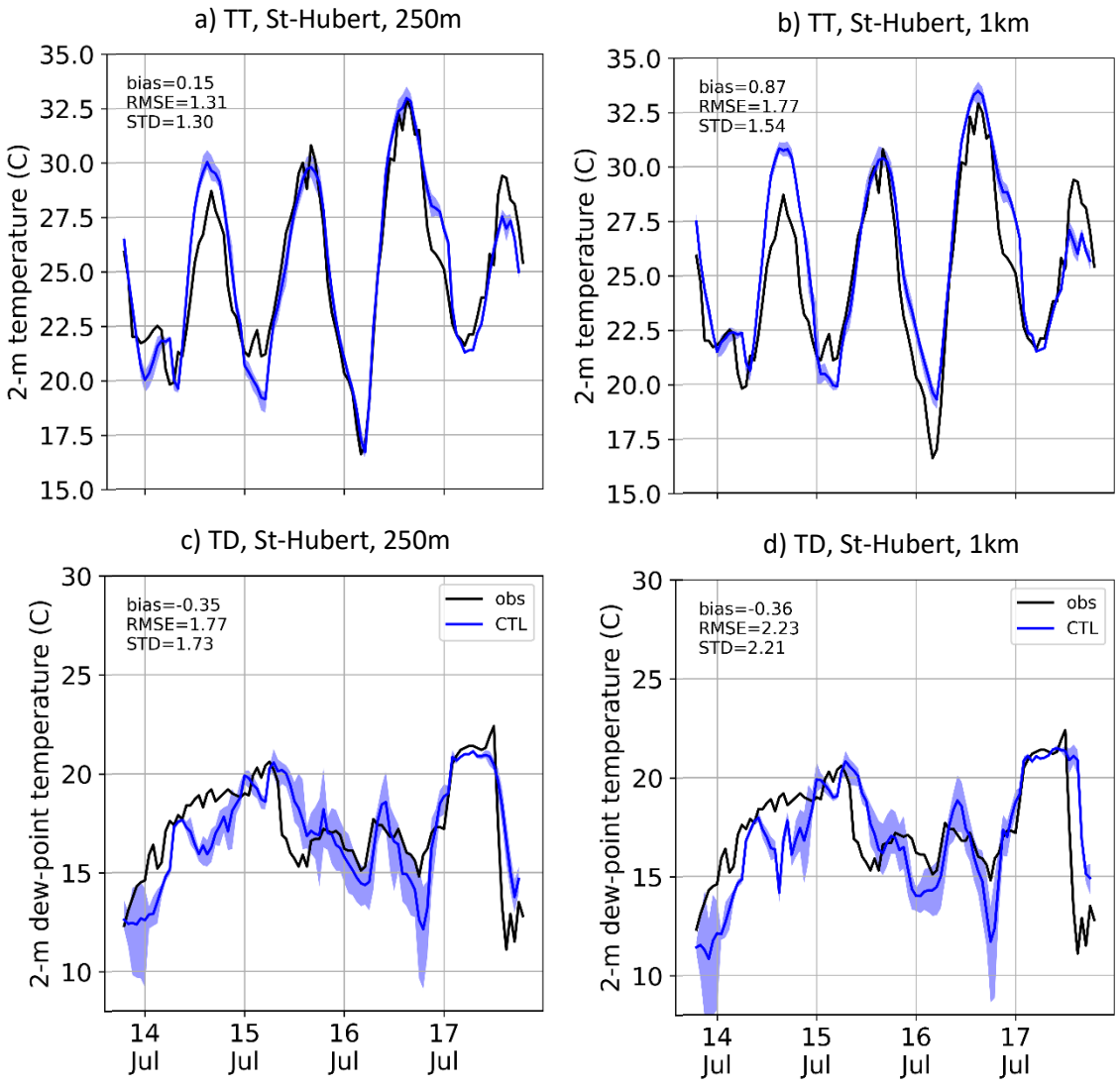

Figure 1.5. **Timeseries of observed and simulated surface variables at St-Hubert for the SYNOPTIC event.** Same as Fig 1.4 but at the St-Hubert station (YHU).

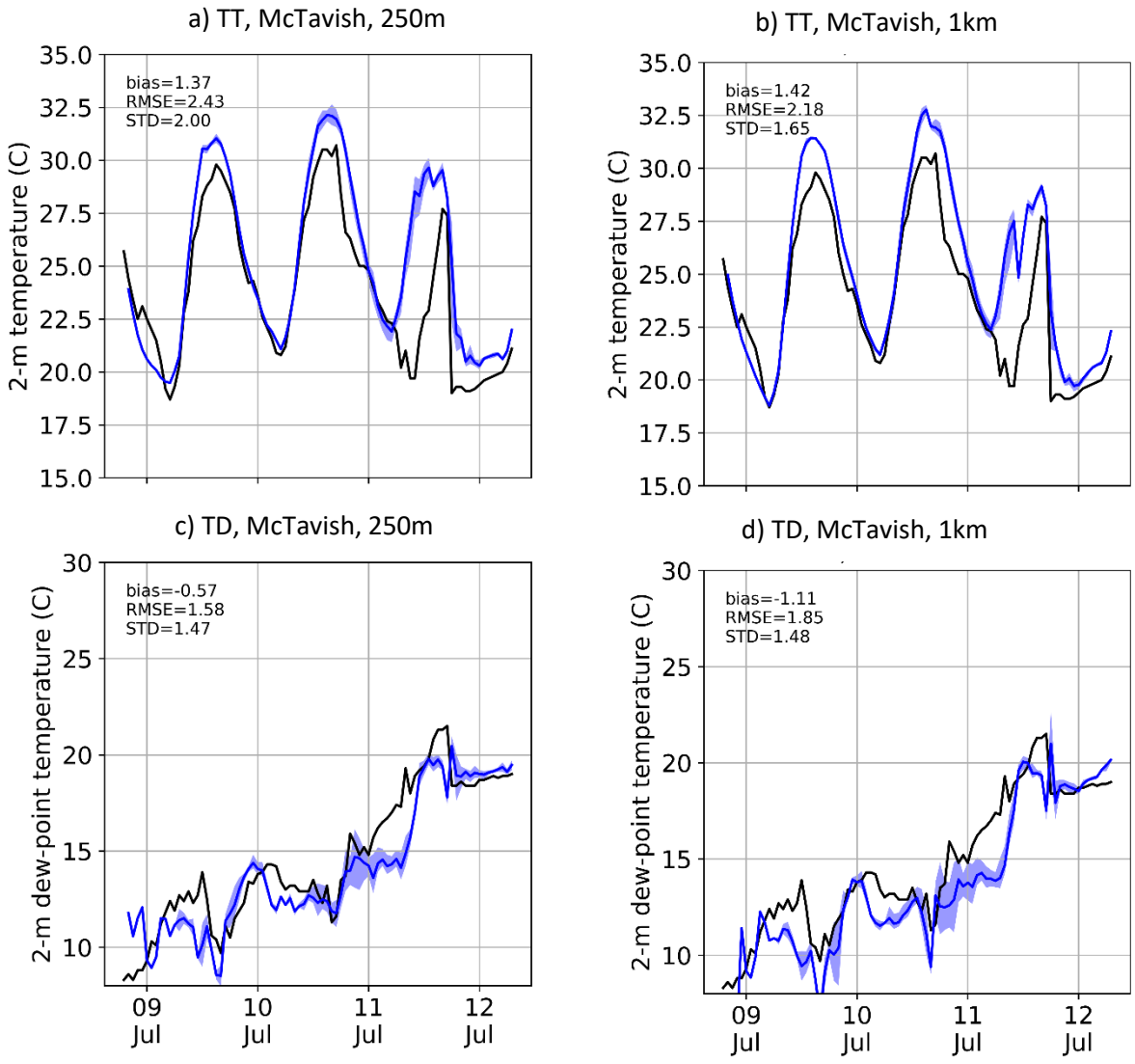

Figure 1.6. **Timeseries of observed and simulated surface variables at McTavish for the SQUALL event.** Observed (black) and simulated (blue) surface air temperature (a,b) and dew point temperature (c,d) at station McTavish (WTA) for the SQUALL event. Left panel are the results of the 250m resolution experiments (a,c) and right panel are the 1km resolution experiments (b,d). The blue shading shows the ensemble spread (5^{th} to 95^{th} percentiles).

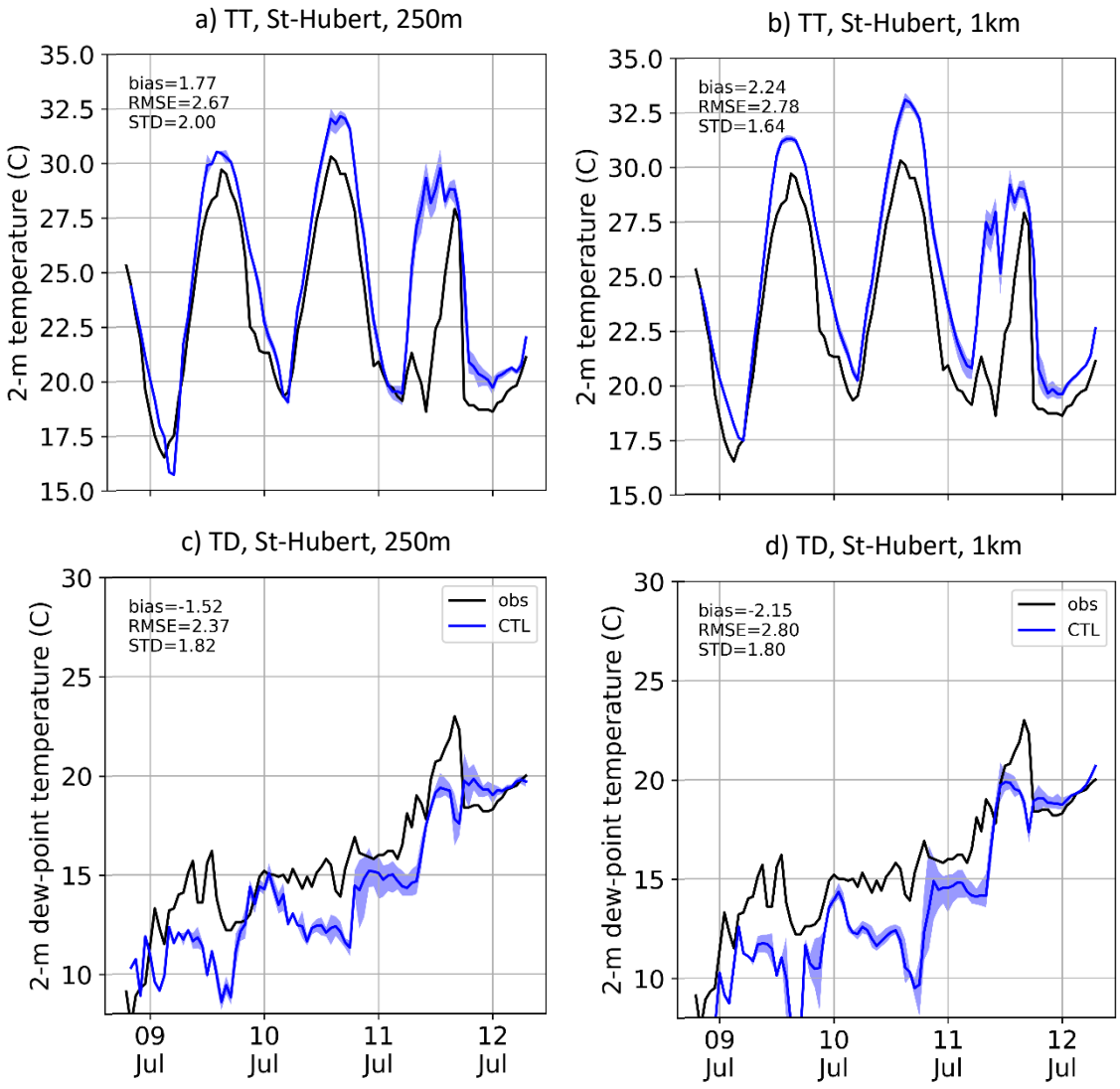

Figure 1.7. **Timeseries of observed and simulated surface variables at St-Hubert for the SQUALL event.** Same as Fig 1.6 but at the St-Hubert station (YHU).

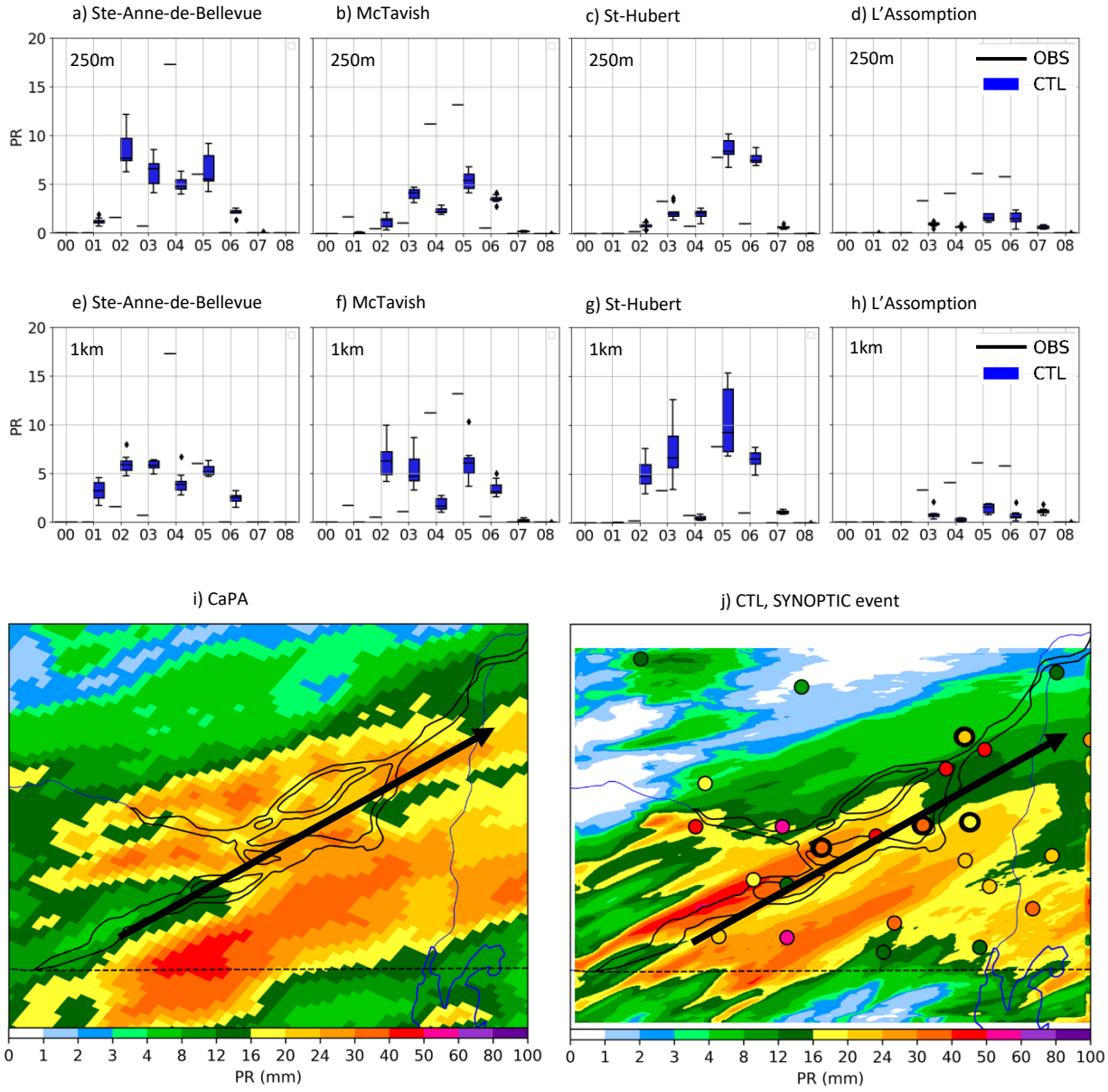

Figure 1.8. **Observed and simulated rainfall for the SYNOPTIC event.** a-d) Timeseries of 1h-precipitation accumulation in four different stations along the precipitation system for the 250 m resolution (a-d) and 1 km resolution (e-h): Ste Anne de Bellevue, up-wind of the city (a,e), McTavish, downtown (b,f), St-Hubert, suburb next to the downtown (c,g) and Assomption, down-wind (d,h). The box represents the 25th to 95th percentile of the ensemble spread, and the whiskers show the rest of the distribution. Outliers are shown with a diamond. Observations are indicated with a black horizontal line. X-axis is the hour on July 17th 2018 (in local time). The bottom panel shows 24-h precipitation accumulation from 2018-07-16 2000 LST to 2018-08-17 2000 LST from CaPA analysis (i) and the ensemble average of CTL run at 250 m (j), with colored circles representing observed accumulation values at available surface stations.

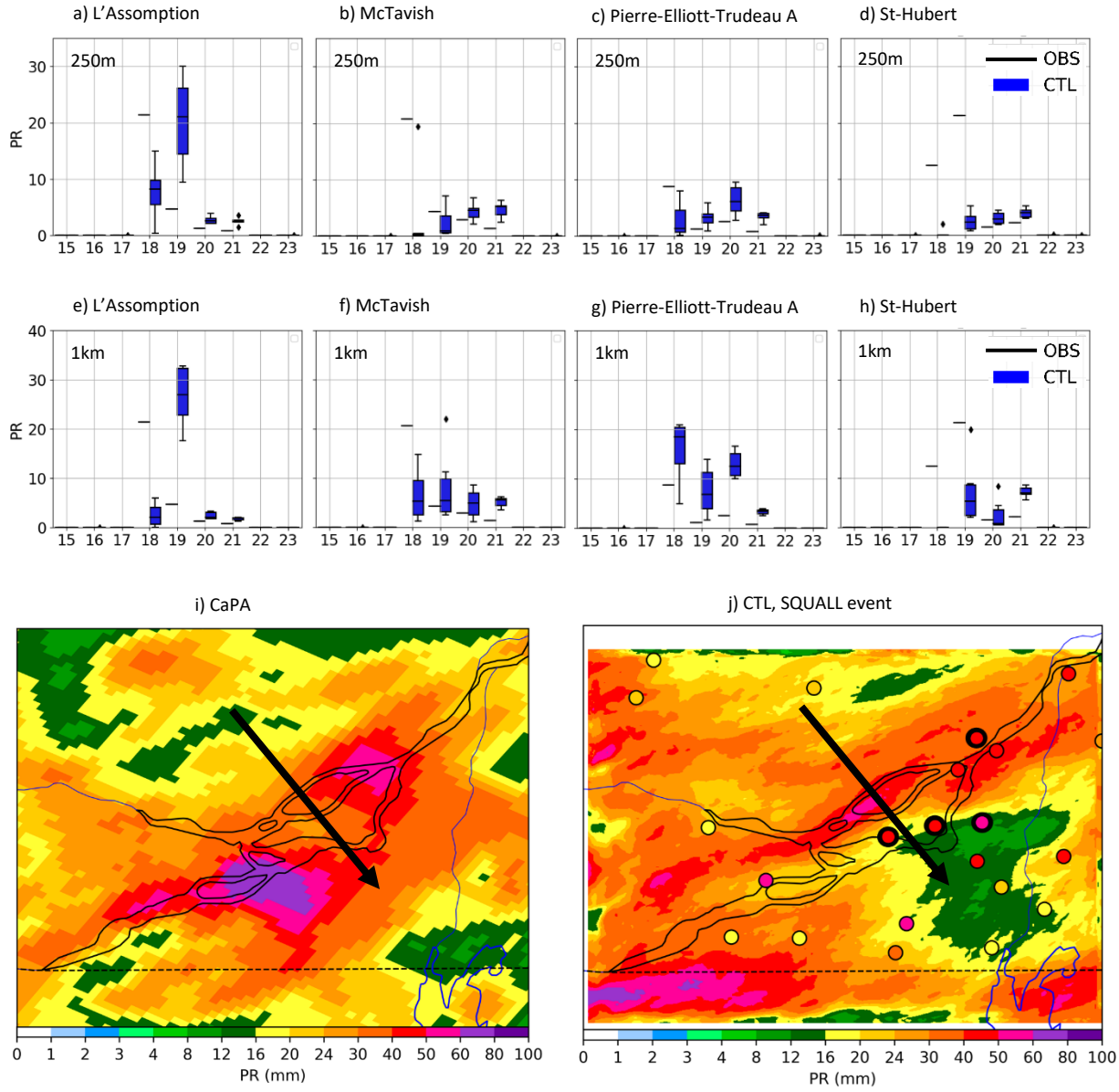

Figure 1.9. **Observed and simulated (ensemble mean) rainfall for the SQUALL event.** a-d) Timeseries of 1h-precipitation accumulation in four different stations along the precipitation system for the 250 m resolution (a-d) and 1 km resolution (e-h): Assomption, up-wind of the city (a,e), McTavish, downtown (b,f), Pierre-Elliott-Trudeau Airport, next to the downtown (c,g) and St-Hubert, down-wind (d,h). The box represents the 25th to 95th percentile of the ensemble spread, and the whiskers show the rest of the distribution. Outliers are shown with a diamond. Observations are indicated with a black horizontal line. X-axis is the hour on July 11th 2019 (in local time). The bottom panel shows 24-h precipitation accumulation from 2019-07-11 0800 LST to 2019-08-12 0800 LST from CaPA analysis (i) and the ensemble average of CTL run at 250 m (j), with colored circles representing observed accumulation values at available surface stations.

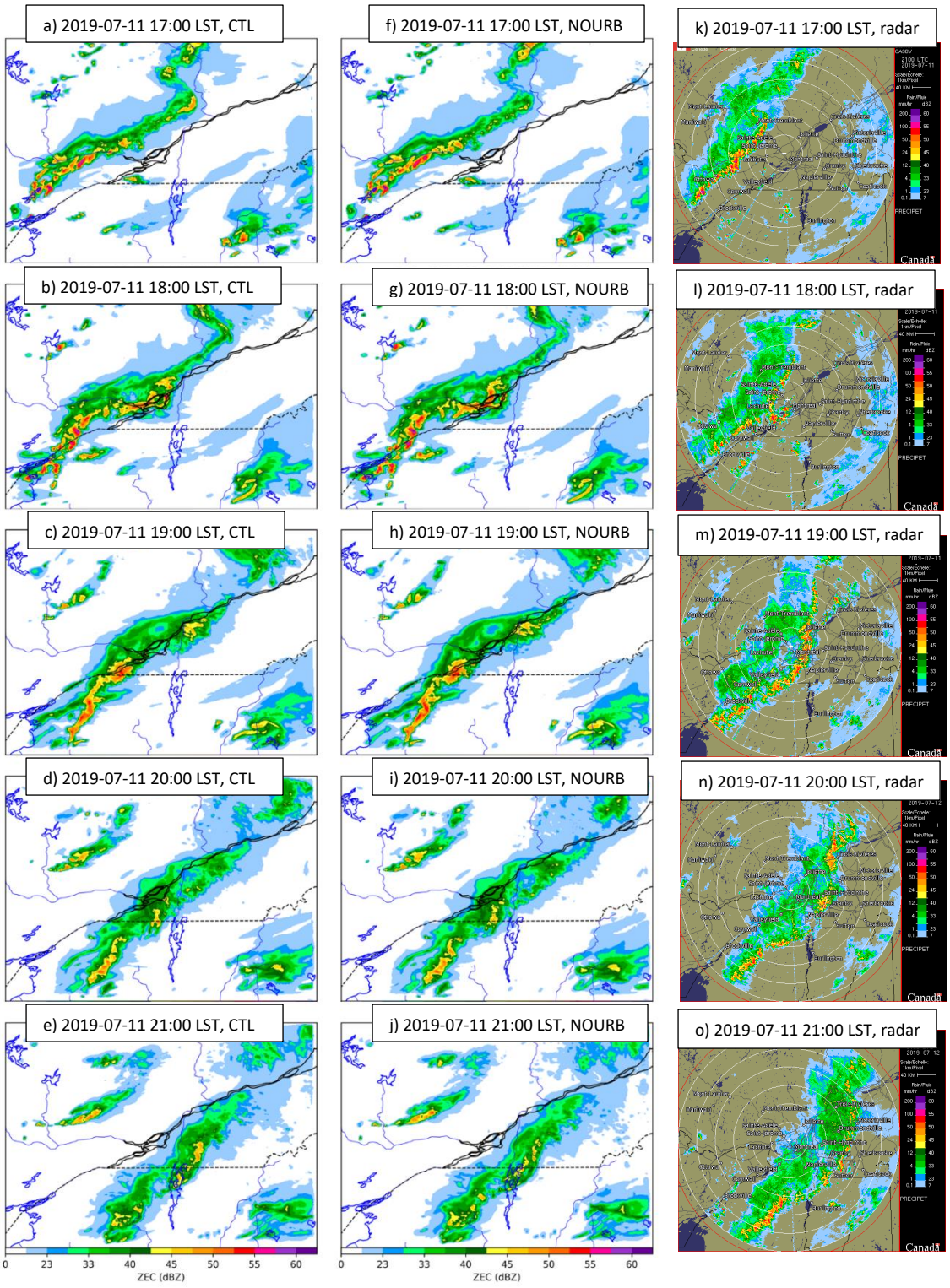

Figure 1.10. **Model reflectivity for SQUALL event.** Maximum reflectivity at different times for the SQUALL event for CTL (left) and NOURB (center) experiment, and from the rader (right). Times are, from top to bottom row, 1800, 1900, 2000, 2100 and 2200 LST on 2019-07-12.

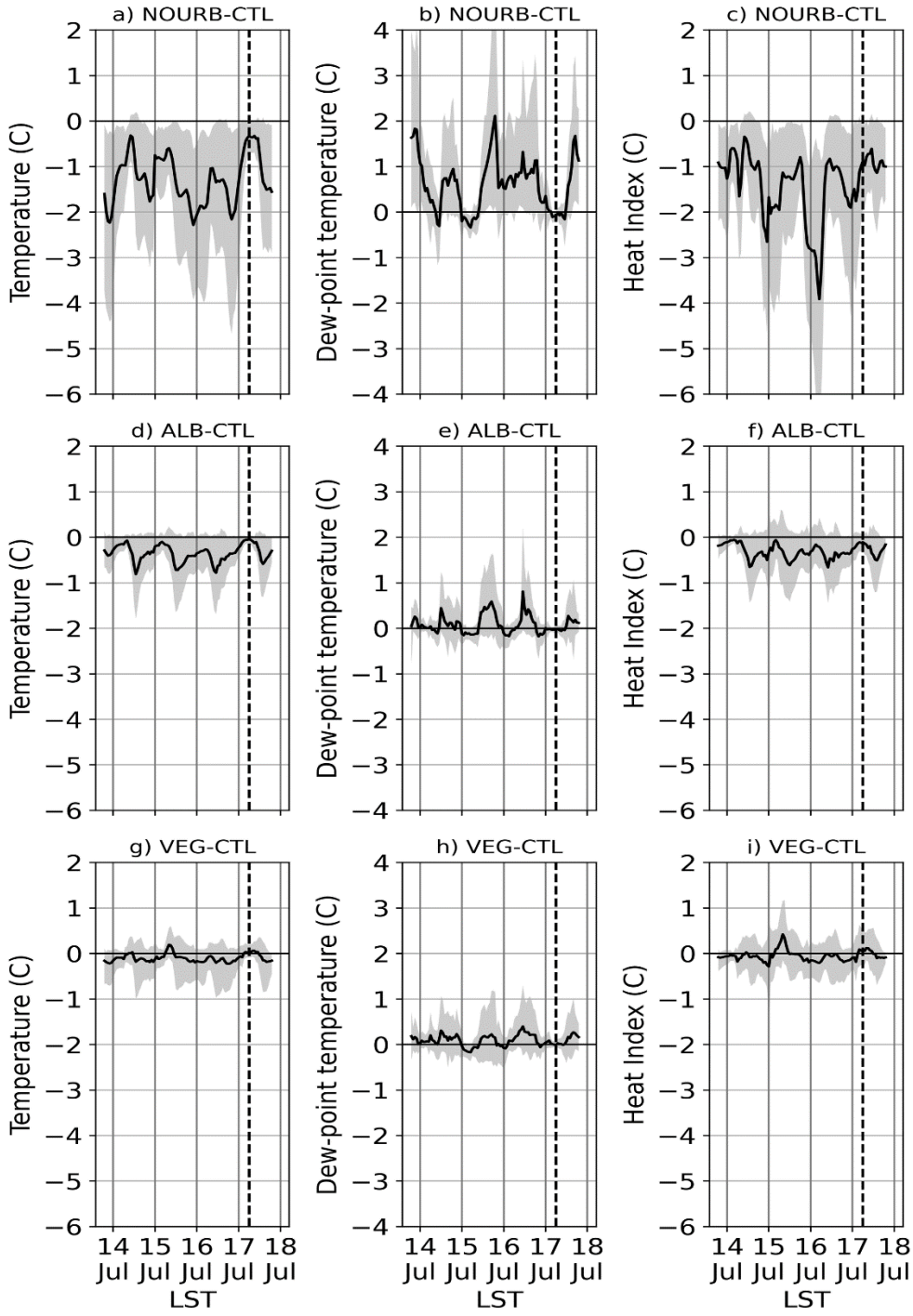

Figure 1.11. **Changes in averaged 2-m air temperature, 2-m dew point and heat index for the SYNOPTIC event.** Spatial timeseries of the difference in 2-m air temperature (a, d, g), 2-m dew point (b, e, h) and heat index (c, f, i) between NOURB-CTL (a, b, c), ALB-CTL (d, e, f) and VEG-CTL (g, h, i) model runs for the SYNOPTIC event. The black line is the spatial average on the island of Montreal of the difference between the sensitivity and the CTL experiments. The gray area is the 5th to 95th percentile and represents the spatial variability on the island of Montreal. The dashed vertical lines show when the precipitation starts.

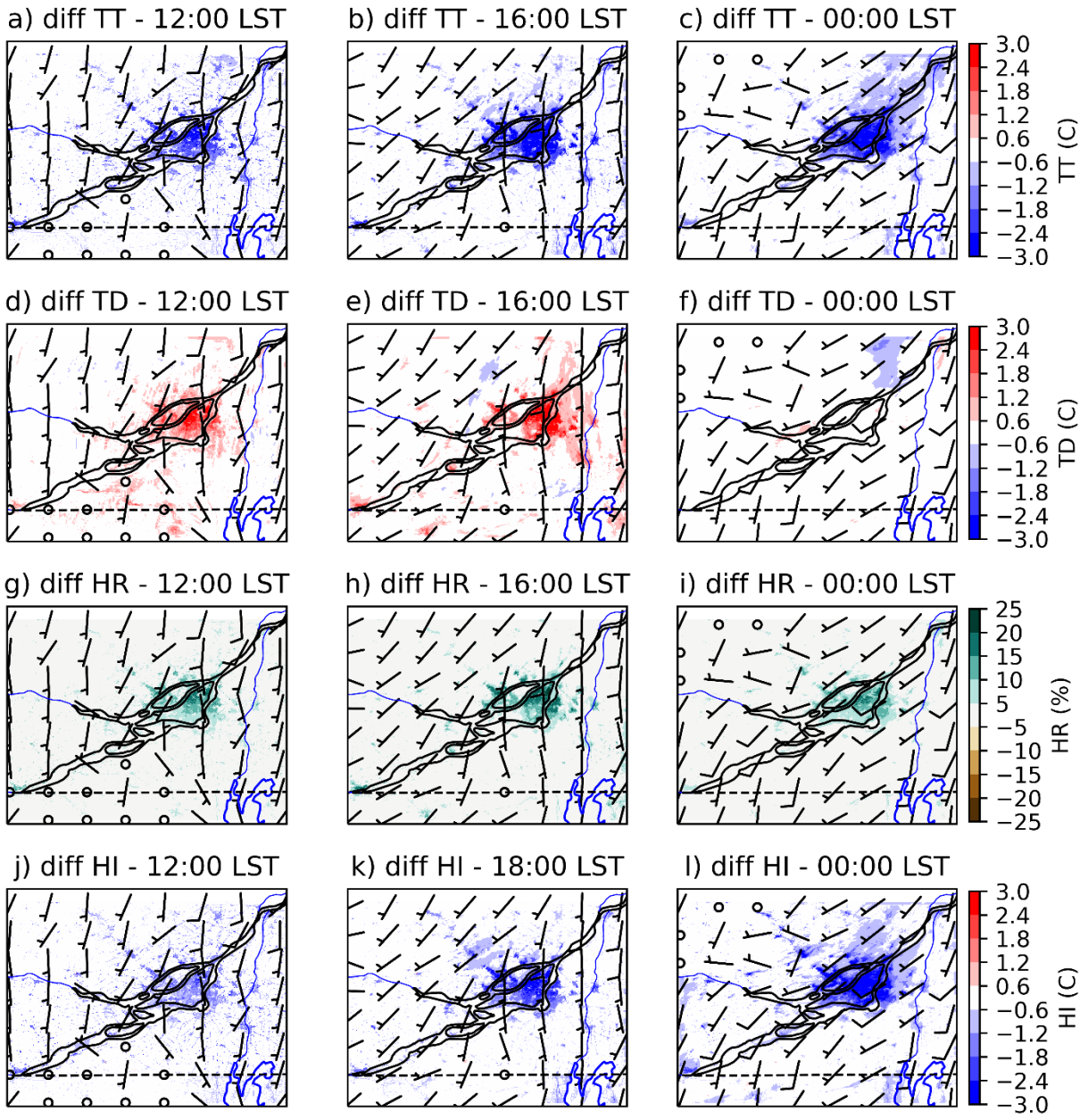

Figure 1.12. **Changes in surface temperature, dew point, relative humidity and heat index between NOURB and CTL for the SYNOPTIC event.** Anomalies in air temperature (a, b, c), dew-point temperature (d, e, f), relative humidity (g, h, i) and heat index (j, k, l) between NOURB and CTL experiments. The three columns correspond to different times: 2018-07-16 12:00 LST (left), 2018-07-16 18:00 LST (center) and 2018-07-17 00:00 LST (right). Surface winds for the CTL experiment are shown (in knots).

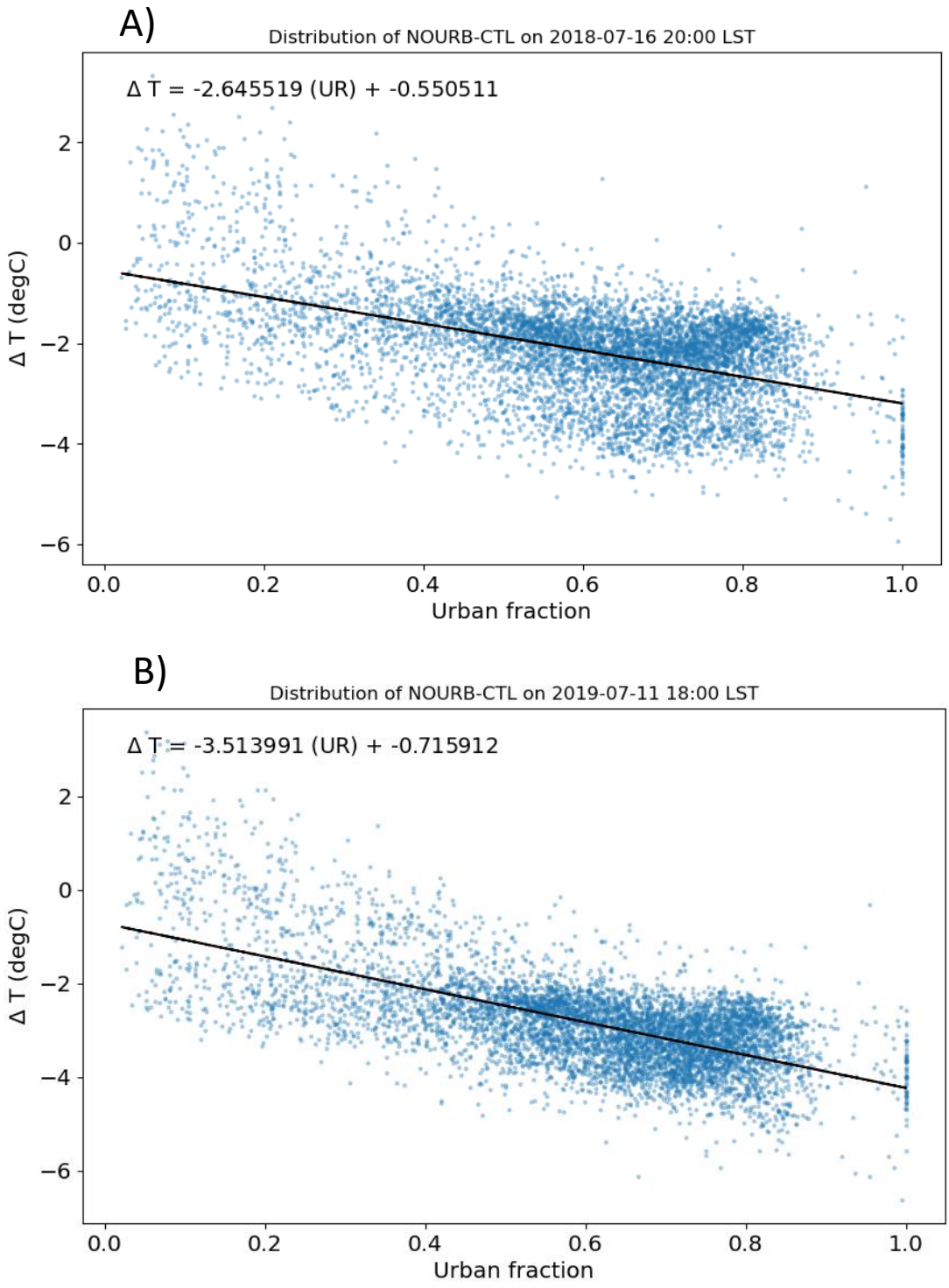

Figure 1.13. **Scatter plots.** Scatter plot of the difference of temperature versus the urban fraction for the SYNOPTIC event at 2018-07-16 20:00 LST (a) and the SQUALL event at 2019-07-11 18:00 LST (b). The black line is the best fitted linear regression, with the corresponding equation on the top.

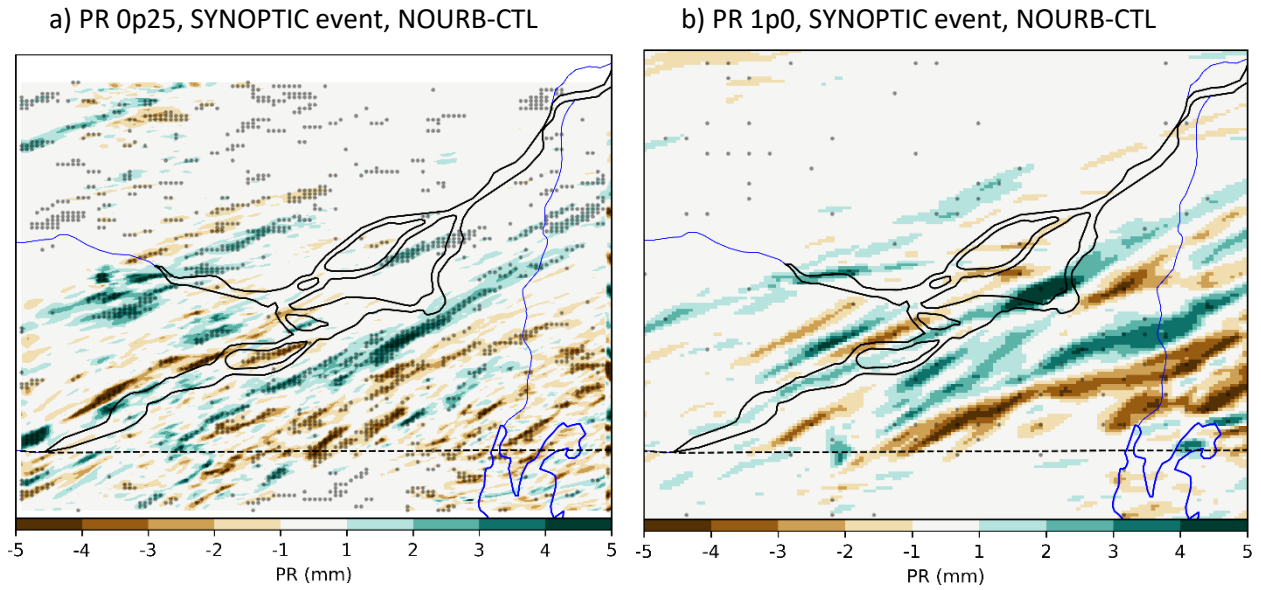

Figure 1.14. **Changes in precipitation for the SYNOPTIC event**. Difference in accumulated precipitation between NOURB and CTL experiments for the 250 m resolution (a) and the 1 km resolution (b). The dots represent gridpoints where the difference are significant (p value = 0.1). Brown signifies more precipitation when the city is present.

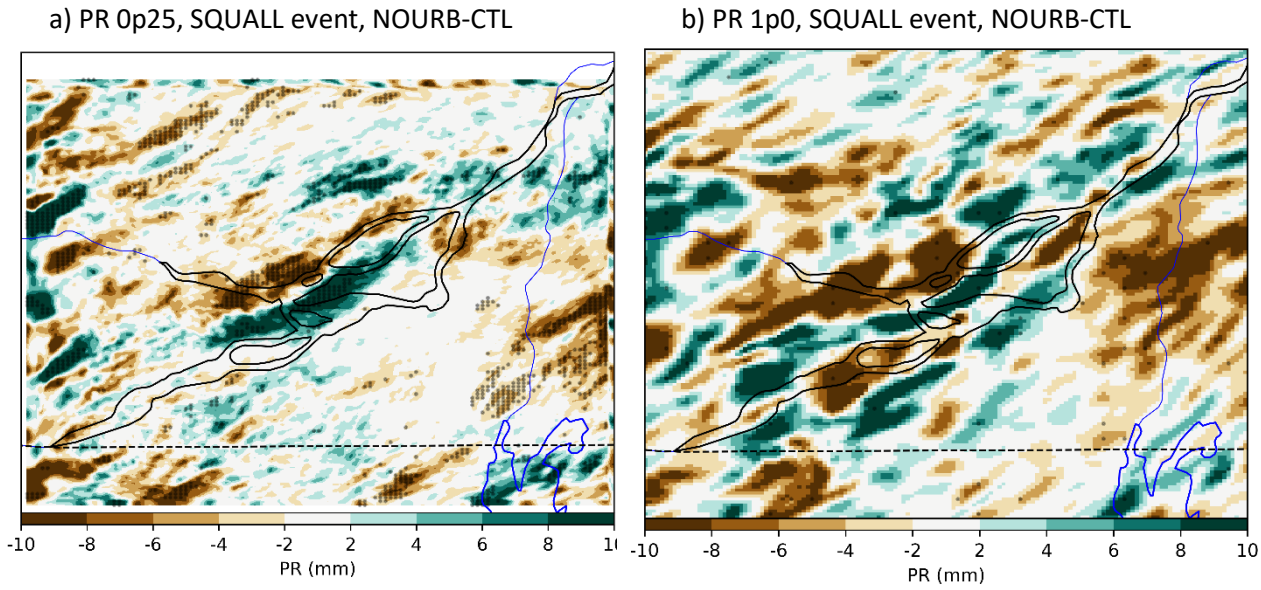

Figure 1.15. **Changes in precipitation for the SQUALL event**. Same as Fig 1.14 but fot the SQUALL event.

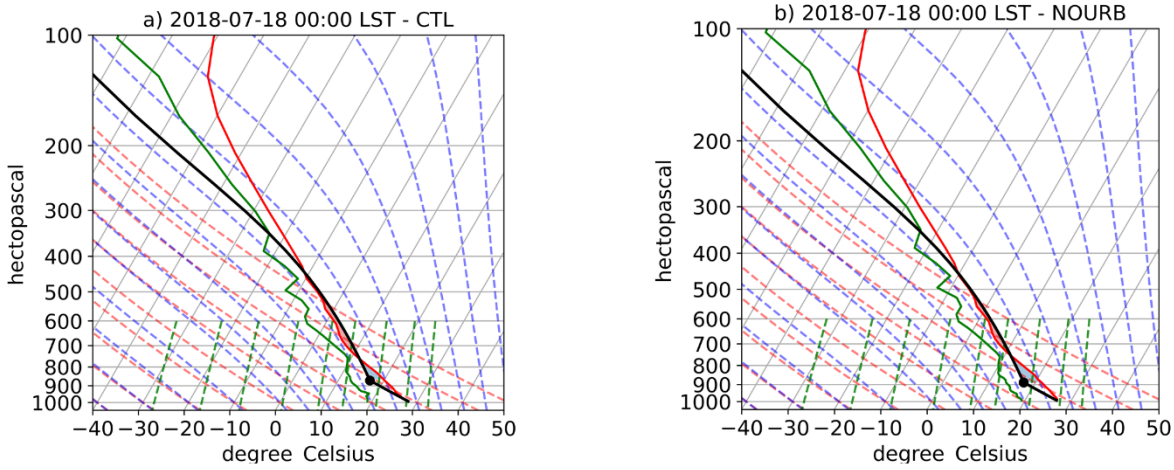

Figure 1.16. **Skew-T diagram for the SYNOPTIC event.** Skew-T diagram on 2018-07-18 00:00 LST for the CTL experiment (a) and NOURB experiment (b) at the closest grid point to McTavish station. The red line is the temperature, the green line is the dew-point temperature and the black line is the air parcel lifted. The blue and red shaded areas represents the layers where convective inhibition (CIN) and convective available potential energy (CAPE) is present, respectively.

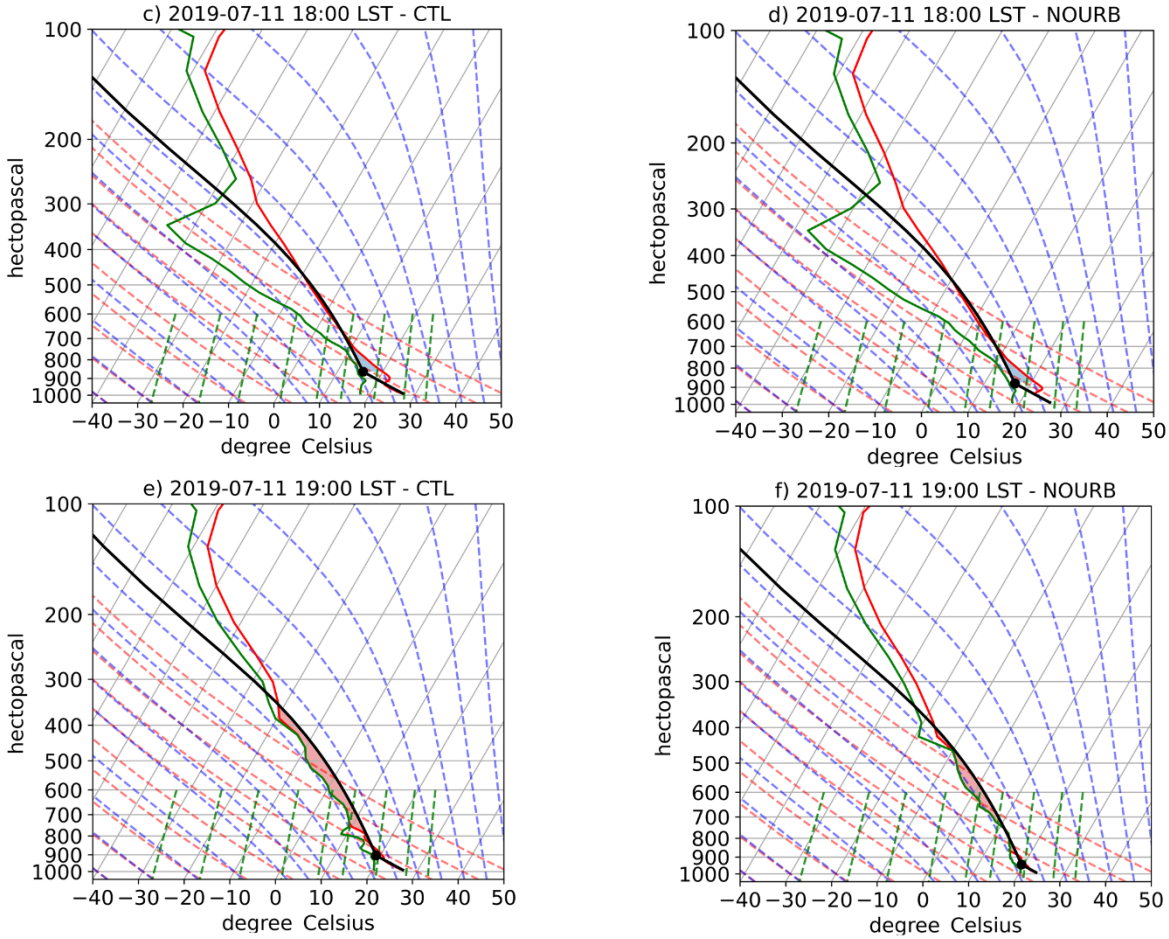

Figure 1.17. **Skew-T diagram for the SQUALL event.** Skew-T diagram on 2019-07-11 18:00 LST (c,e) and 2019-07-11 19:00 LST (d,f) for the CTL experiment (c,e) and NOURB experiment (d,f) at the closest grid point to McTavish station. The red line is the temperature, the green line is the dew-point temperature and the black line is the air parcel lifted. The blue and red shaded areas represents the layers where convective inhibition (CIN) and convective available potential energy (CAPE) is present, respectively.

CONCLUSION

L'objectif de ce travail est de déterminer les effets potentiels de la présence et de la composition de la ville de Montréal sur le climat local. Plusieurs études ont investigué l'ICU dans la région de Montréal (Oke & Maxwell, 1975; Wang & Akbari, 2016) et l'efficacité de certaines stratégies d'atténuation de l'ICU (Leroyer et al., 2019), mais peu ont investigué l'impact de l'ICU sur la précipitation estivale. Pour y arriver, des expériences numériques de prévision du temps à très haute résolution (250 m) sont effectuées dans la région. Les expériences utilisent le modèle atmosphérique global environnemental multiéchelles (GEM) et le schéma de surface *Town Energy Balance* (TEB) et se basent sur la configuration utilisée dans plusieurs études sur le climat urbain à Environnement et Changement climatique Canada (ECCC) (Leroyer et al., 2022). Deux études de cas ont été effectuées : un système de grande échelle en 2018 (SYNOPTIC) et une ligne de grain en 2019 (SQUALL).

D'une part, les processus de surface semblent généralement bien représentés par le modèle. La température de l'air et la température du point de rosée à la surface suivent généralement les observations disponibles. Les températures maximales journalières du modèle numérique sont légèrement plus élevées que celles observées. Ceci peut être associé au fait que les observations sont effectuées en un seul point au-dessus d'une zone herbacée, alors que le modèle numérique donne une moyenne sur une région de 250 m x 250 m. D'autre part, tant pour l'évènement SYNOPTIC que celui de SQUALL, le modèle simule de la pluie, mais selon un patron et une intensité différente que les observations. Dans les deux cas étudiés, les quantités d'accumulations de précipitation calculées par le modèle sont plus faibles au-dessus et en aval du centre-ville, ce qui suggère un blocage des systèmes par la ville dans les expériences numériques.

La comparaison de l'expérience NOURB, dans laquelle toutes les surfaces urbaines sont remplacées par de la végétation basse, avec l'expérience CTL montre l'intensité des modifications induites par la ville sur le climat local. Dans NOURB, le confort est grandement amélioré, avec l'indice de chaleur calculé qui diminue de 2 à 4°C en moyenne durant la nuit, et de 1°C durant le jour. Toutefois, une grande variabilité spatiale de l'indice de chaleur dans la région de Montréal est simulée. Les zones urbaines denses présentent une diminution de l'indice de chaleur de l'ordre de 4 à 6°C pendant la nuit alors que l'effet est plutôt négligeable dans les parcs et dans les zones rurales. Les anomalies simulées sont cohérentes avec les différences observées de températures entre la station située en milieu urbain (McTavish, WTA) et celles

situées en milieu rural (Mirabel, YMX et Saint-Hubert, YHU), où les différences atteignent 5°C durant la nuit. Ainsi, l'ICU dans la région de Montréal est important et les stratégies d'atténuation de l'ICU ont le potentiel d'améliorer le confort ressenti par les Montréalais.

Deux scénarios d'atténuation sont étudiés et présentés dans ce mémoire : 1) l'augmentation de l'albédo des surfaces urbaines (ALB) et 2) l'ajout de végétation basse au niveau de la rue (VEG). Premièrement, l'expérience où l'albédo est augmenté montre une réduction de la température de surface de l'air par rapport à l'expérience de CTL. Cette réduction est maximale quand le rayonnement solaire incident est maximal (l'après-midi) et négligeable quand le rayonnement est nul (la nuit). Le bilan hydrique n'est pas modifié par l'augmentation de l'albédo. Ainsi, cette stratégie améliore le confort thermique de l'ordre de 0.5 à 1°C durant le jour seulement, amélioration qui est liée à la réduction de la température. Deuxièmement, l'impact du remplacement d'une partie des routes par de la végétation basse (VEG) est généralement faible. En moyenne, la température semble légèrement plus faible dans l'expérience VEG que dans l'expérience CTL, mais l'humidité, quant à elle, est légèrement plus élevée. Ces deux variables influencent de manière opposée l'indice de chaleur, qui semble plus élevé dans certaines régions et plus faible dans d'autres, avec une moyenne spatiale proche de zéro. Une analyse spatiale des résultats indique que l'indice de chaleur est diminué dans les zones urbaines denses. Ceci indique que malgré de la vapeur d'eau ajoutée dans l'air, la diminution de température est assez importante dans les zones denses pour être bénéfique sur le confort ressenti. L'ajout d'arbres au lieu de végétation basse aurait certainement un plus grand impact sur le confort thermique puisqu'ils créent des zones ombragées à la surface (Krayenhoff et al., 2020). Ce scénario n'a pas pu être considéré dans cette étude puisque le schéma urbain employé ne permet pas la représentation de cet effet. Une investigation avec d'autres schémas urbains où l'effet des arbres dans le canyon est pris en compte fournirait de meilleures informations sur cette stratégie d'atténuation (Lemonsu et al., 2012).

Les résultats obtenus avec les scénarios d'atténuation présentés dans ce mémoire suivent les résultats d'une étude similaire effectuée à Montréal pour les autorités locales (Leroyer et al., 2019), où plusieurs scénarios d'atténuation de l'ICU sont analysés. De plus, Leroyer et al. (2019) ont montré que la faible diminution de la température (< 0.5°C) associée à l'ajout de la végétation basse dans les rues pouvait être diminuée davantage (autour de 1°C) en forçant l'irrigation du sol. Finalement, une combinaison de l'augmentation de l'albédo, qui réduit la température durant le jour, et de l'ajout de la végétation, qui réduit la température durant la nuit, pourrait être davantage bénéfique à réduire l'intensité de l'ICU.

Quant à la précipitation de l'évènement SYNOPTIC, où un système à grande échelle traverse la ville durant la nuit, l'impact sur la précipitation causé par la présence de la ville n'est pas détecté dans nos expériences numériques. Ceci est possiblement dû au fait que la modification de la masse d'air au-dessus de la ville due à l'ICU n'est pas assez importante pour affecter un système bien organisé et de grande envergure. Les trajectoires et intensités de ces types de systèmes sont définies par des facteurs à l'échelle synoptique, ainsi, une faible perturbation à la surface a probablement peu d'impact, comme le démontre nos résultats. De plus, bien que le signal de l'ICU soit à son plus fort durant la nuit, l'atmosphère est typiquement très stable comparativement au jour, où la surface très chaude entraîne une importante instabilité verticale. Ces deux mécanismes expliquent pourquoi nos résultats montrent peu de différences sur la précipitation entre les expériences CTL et NOURB. Cependant, Li et al. (2020) ont montré que, dans certains cas, l'ICU a un impact significatif sur la stabilité atmosphérique et par conséquent, augmente les quantités de précipitation. C'est pour cela qu'un deuxième évènement de précipitation, en 2019, est étudié. Contrairement à l'évènement SYNOPTIC, celui de 2019 est caractérisé par une grande instabilité : une ligne de grain se développe dans le nord-ouest de l'île de Montréal et traverse celle-ci à la fin de l'après-midi. Dans ce cas, nos résultats montrent un faible impact sur le système et les précipitations accumulées. Plus de pluie au-dessus de la ville est obtenue dans l'expérience CTL comparativement à NOURB. De plus, le motif spatial de précipitation accumulée est différent entre les deux expériences, ce qui signifie un impact possible de la surface urbaine. Quand la ville est présente (CTL), le système semble bloqué en amont de Montréal avant de se séparer en plus petites cellules orageuses. Finalement, l'analyse du profil vertical de l'atmosphère au-dessus du centre-ville de Montréal montre une région de CAPE assez grande juste avant le passage du système, indiquant l'instabilité de l'atmosphère à ce moment. Cette région de CAPE est légèrement plus grande dans l'expérience CTL que dans NOURB, indiquant que l'ICU accroît l'instabilité et la convection, et par conséquent a plus de possibilités d'intensifier l'orage. Par contre, dans l'expérience numérique, la ligne de grain se sépare et s'affaiblit avant de traverser la ville, ce qui peut expliquer pourquoi l'impact sur la précipitation est faible. Malgré tout, ces résultats mettent en évidence comment la présence d'une zone urbaine affecte la stabilité verticale de l'atmosphère surtout pendant les périodes de haute instabilité (comme la fin de l'après-midi), et montrent comment la ville de Montréal a la possibilité d'affecter la précipitation.

L'étude présentée dans ce mémoire supporte les résultats obtenus par Li et al. (2020), qui suggèrent une augmentation de la précipitation due à l'ICU. Par contre, les résultats présentés ci-dessus indiquent aussi que les conclusions sur la modification de la précipitation par les zones urbaines obtenues par des études

de cas isolées doivent être interprétées avec précaution, puisque la précipitation est déterminée par de multiples conditions météorologiques. Ainsi, d'autres évènements doivent être étudiés afin d'avoir une compréhension plus robuste de la précipitation urbaine. De plus, une différente configuration du modèle ou l'utilisation de différents modèles atmosphériques pourraient aider à déterminer les incertitudes et fausses représentations de la pluie par les modèles numériques.

Finalement, il faut noter que Montréal a une position géographique particulière puisque la ville est comprise sur une île située dans une vallée. Il est de croyance commune que Montréal a tendance à bloquer ou faire bifurquer les systèmes venant de l'ouest de part et d'autre de l'île. Un bon exemple de ce phénomène fut visible en 2022, quand un derecho provenant de l'ouest s'est séparé en deux à l'approche de l'île de Montréal, qui fut épargnée de l'orage. Des météorologues commentant l'évènement expliquent que le fleuve modifie la divergence dans les bas niveaux, ce qui protège la ville d'orages violents (Ouellette-Vézina, 2022). Bien que les évènements choisis dans cette étude étaient des systèmes qui traversaient bel et bien la ville, les résultats obtenus par le modèle tendent à supporter ce phénomène. Lors de l'évènement SQUALL, les observations montrent une certaine séparation et bifurcation de la ligne de grain à l'approche de la ville, qui est recombinée au-dessus de la ville. Le modèle réussit à obtenir cette séparation, mais n'arrive pas à reformer le système par la suite. Ce comportement du modèle indique peut-être une surestimation des processus qui influencent la séparation des systèmes. Par conséquent, des études supplémentaires sur la sensibilité du modèle aux propriétés du fleuve (température, présence, etc.) sont nécessaires afin de comprendre le rôle de Montréal sur la bifurcation des orages.

ANNEXE A

MATÉRIEL SUPPLÉMENTAIRE COMMUN

Table S1. Weather stations. Information and localisation of weather stations used as observations.

Identifier	Station name	Latitude	Longitude	Type
WTA	McTavish	45.50°N	73.58°W	Hourly
YHU	St-Hubert Airport	45.52°N	73.42°W	Hourly
YUL	Pierre-Elliott-Trudeau Airport	45.47°N	73.74°W	Hourly
WJT	St-Jovite	46.08°N	74.56°W	Hourly
YMX	Mirabel	45.67°N	74.03°W	Hourly
WEW	Assomption	45.81°N	73.43°W	Hourly
WVQ	Saint-Anne de Bellevue	45.43°N	73.93°W	Hourly
MGB	Granby	45.37°N	72.78°W	Hourly
WIT	Ste-Clothilde	45.17°N	73.68°W	Hourly
WIZ	Acadie	45.29°N	73.35°W	Hourly
WBZ	St-Anicet	45.12°N	74.29°W	Hourly
7015730	Oka	45.50°N	74.07°W	Daily
7024100	Laprairie	45.38°N	73.43°W	Daily
7028700	Vercheres	45.77°N	73.37°W	Daily
7026612	Rivière-des-Prairies	45.30°N	74.05°W	Daily
7014290	Les Cèdres	45.40°N	73.13°W	Daily
7024627	Marieville	45.80°N	74.05°W	Daily
7037400	St-Jerome	45.32°N	74.17°W	Daily
7011947	Coteau-du-lac	45.65°N	74.33°W	Daily
7033650	Lachute	45.50°N	74.37°W	Daily
7016470	Rigaud	45.30°N	74.05°W	Daily
7026734	Sabrevois	45.22°N	73.20°W	Daily
7023075	Hemmingford	45.07°N	73.72°W	Daily
7026916	Lacolle	45.08°N	73.38°W	Daily
7025745	Ormstown	45.12°N	74.05°W	Daily
7037310	St-Hippolyte	45.98°N	74.00°W	Daily
7028200	Sorel	46.03°N	73.12°W	Daily
7037310	Arundel	45.95°N	74.62°W	Daily

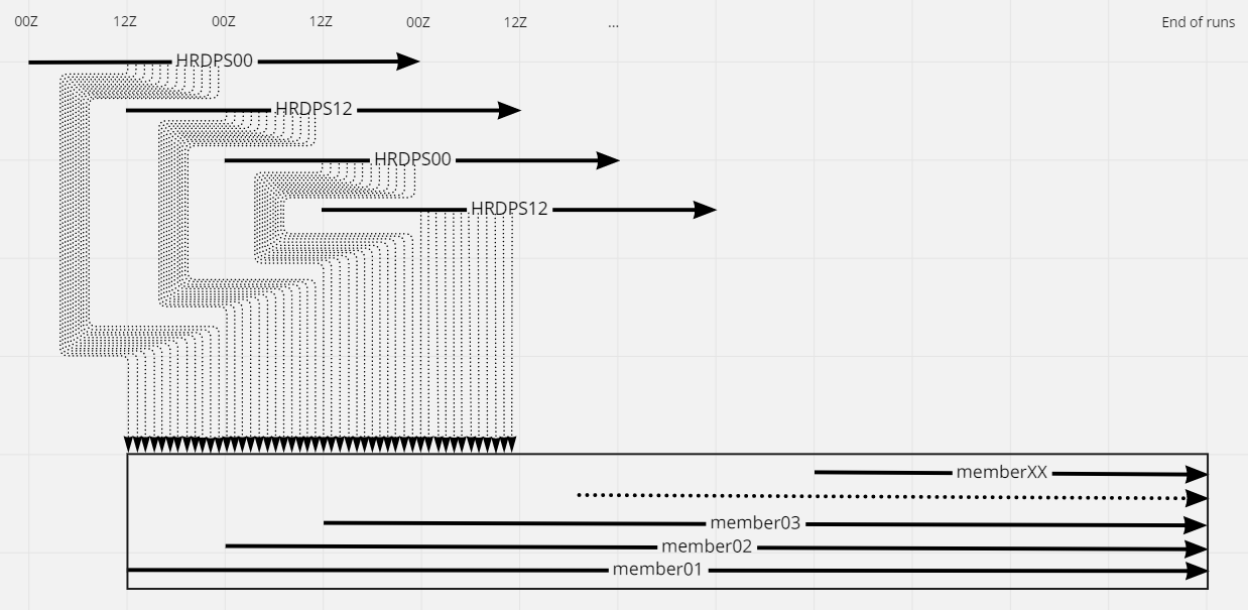

Figure A.1. **Driving data ensemble.** The ensemble driving data from the 2.5-km HRDPS forecast.

ANNEXE B

MATÉRIEL SUPPLÉMENTAIRE COMMUN

A) 02:00 LST B) 03:00 LST

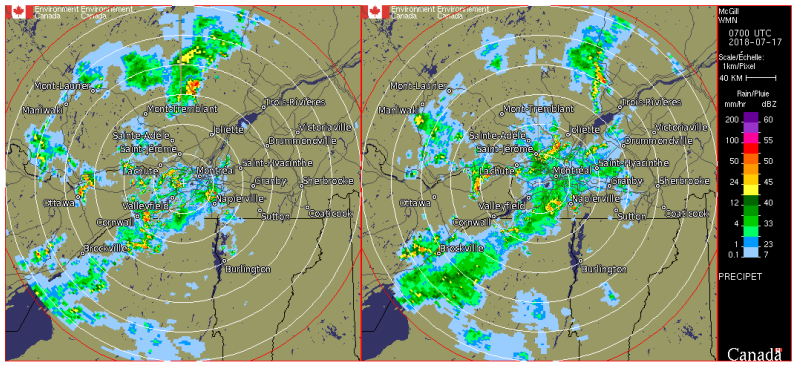

C) 04:00 LST D) 05:00 LST

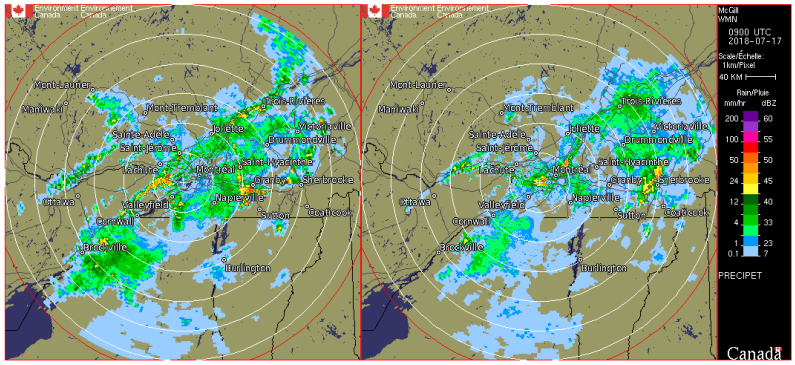

E) 06:00 LST F) 07:00 LST

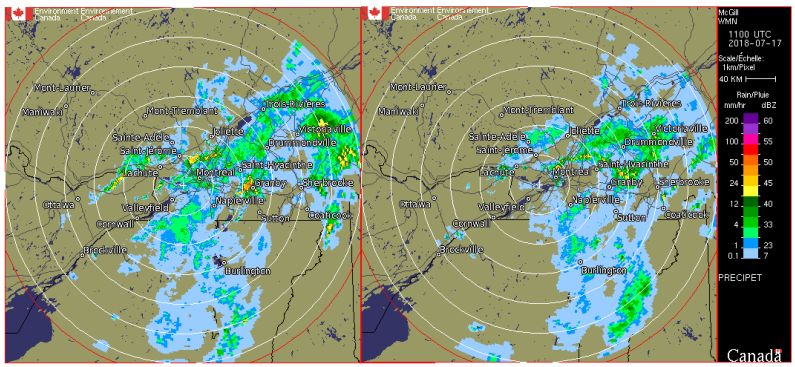

Figure B.1.**Radar images for the SYNOPTIC event.** Radar images from the Blainville radar on 2018-07-17 at a) 0200 LST (0600 UTC), b) 0300 LST (0700 UTC), c) 0400 LST (0800 UTC), d) 0500 LST (0900 UTC), e) 0600 LST (1000 UTC) and f) 0700 LST (1100 UTC). The island of Montreal is located southeast from the center of the radar (see label).

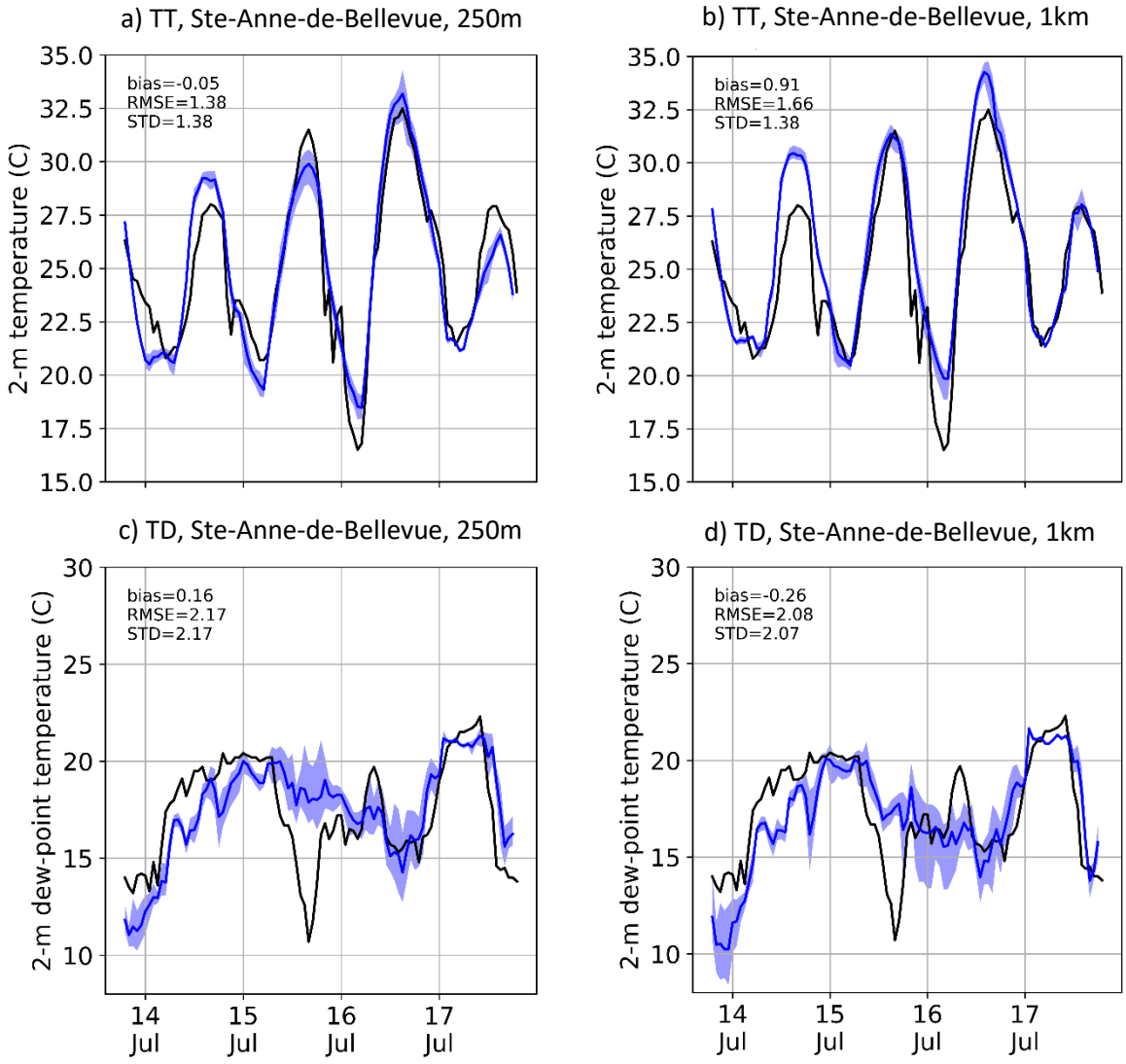

Figure B.2.**Timeseries of observed and simulated surface variables at Ste-Anne-de-Bellevue for the SYNOPTIC event.** Same as Fig 1.4, but for Ste-Anne-de-Bellevue (WVQ) station.

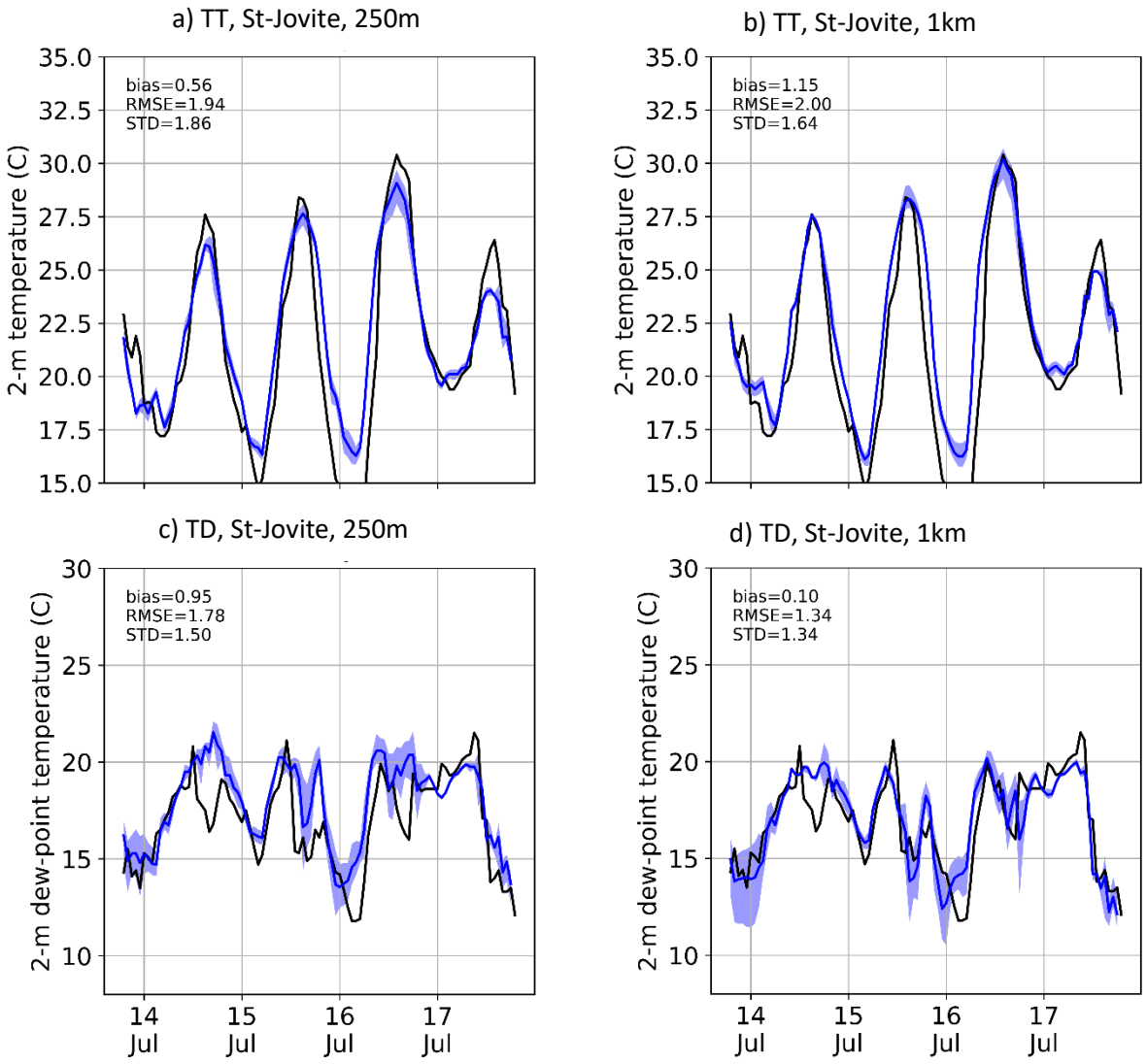

Figure B.3. **Timeseries of observed and simulated surface variables at St-Jovite for the SYNOPTIC event.** Same as Fig 1.4, but for St-Jovite (WJT) station.

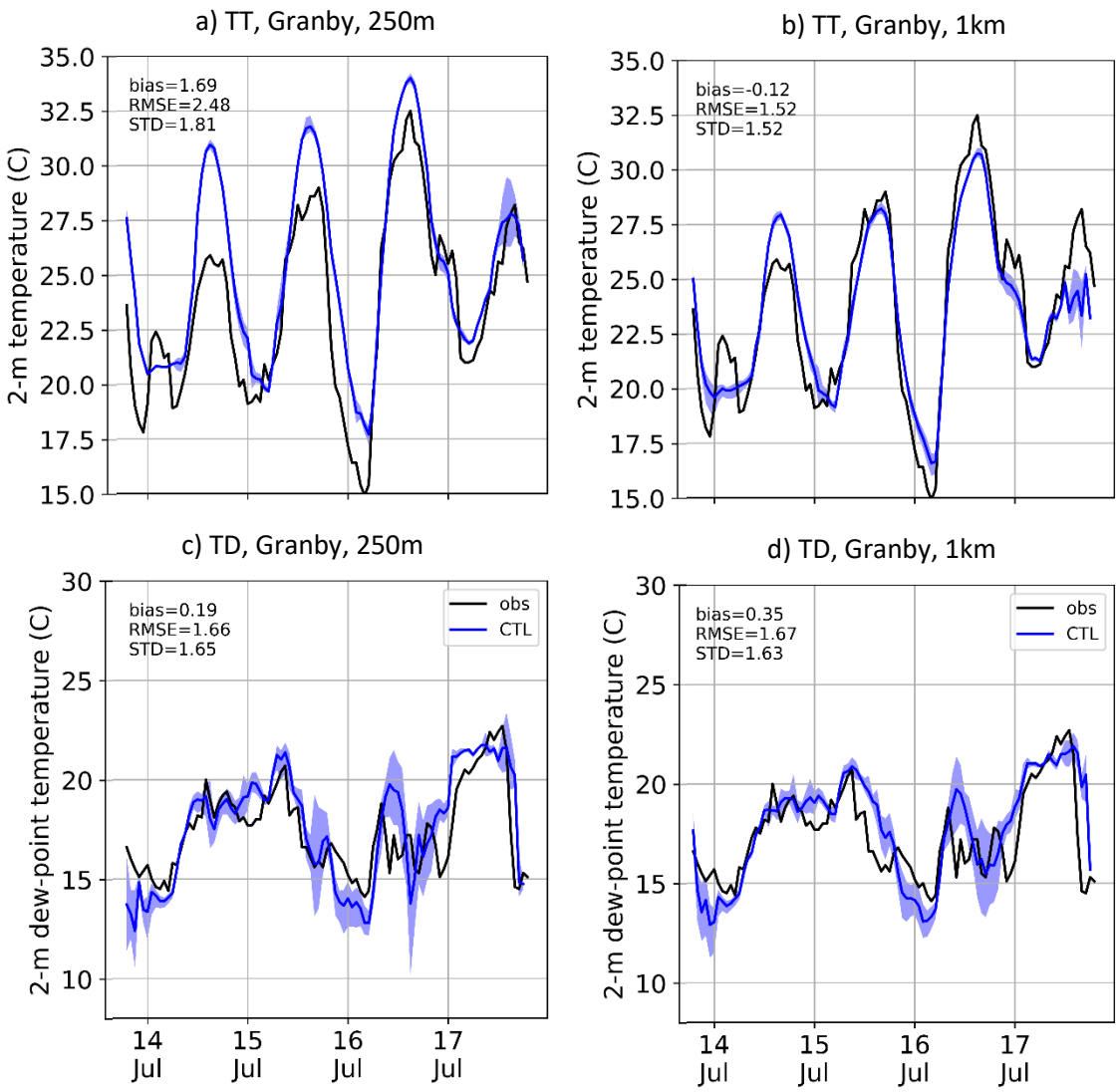

Figure B.4. **Timeseries of observed and simulated surface variables at Granby for the SYNOPTIC event.** Same as Fig 1.4, but for Granby (MGB) station.

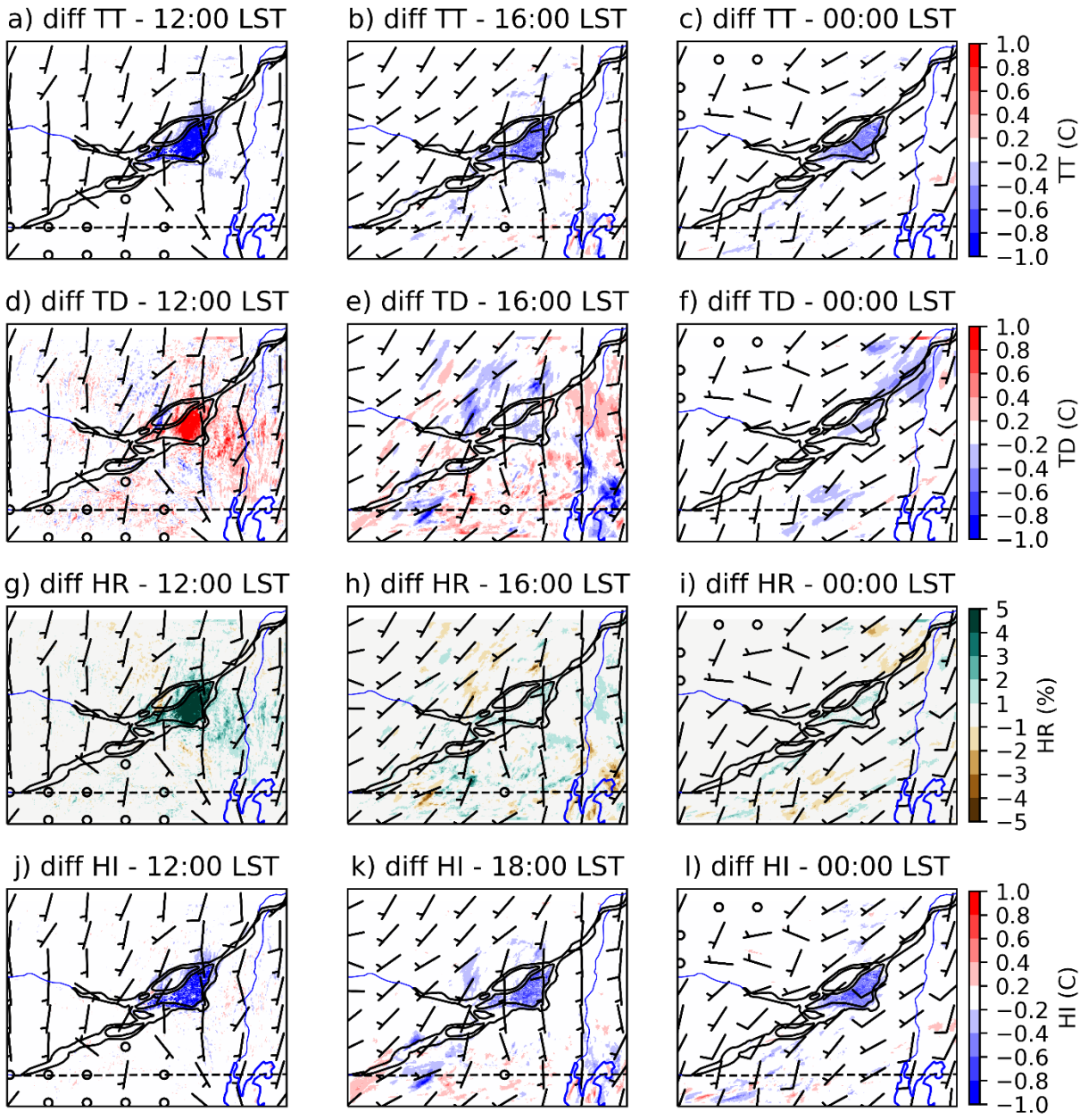

Figure B.5. **Changes in surface temperature, dew point, relative humidity and heat index between ALB and CTL for the SYNOPTIC event.** Same as Fig 1.12, but for the ALB experiment. Anomalies in air temperature (a, b, c), dew-point temperature (d, e, f), relative humidity (g, h, i) and heat index (j, k, l) between ALB and CTL experiments. The three columns correspond to different times: 2018-07-16 12:00 LST (left), 2018-07-16 18:00 LST (center) and 2018-07-17 00:00 LST (right). Surface winds for the CTL experiment are shown (in knots).

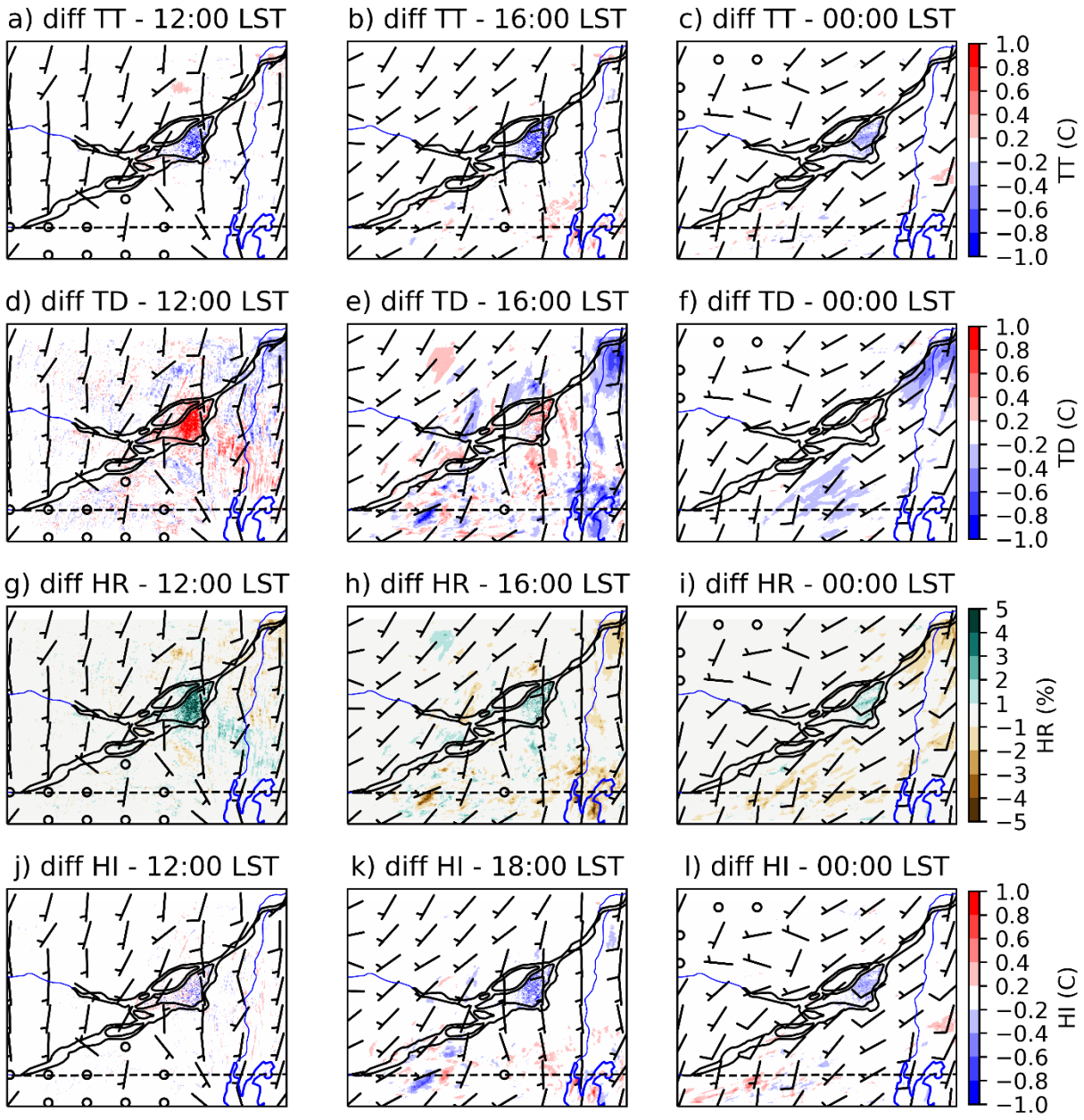

Figure B.6**. Changes in surface temperature, dew point, relative humidity and heat index between VEG and CTL for the SYNOPTIC event.** Same as Fig 1.12, but for the VEG experiment.

ANNEXE C

MATÉRIEL SUPPLÉMENTAIRE POUR L'ÉVÈNEMENT SQUALL

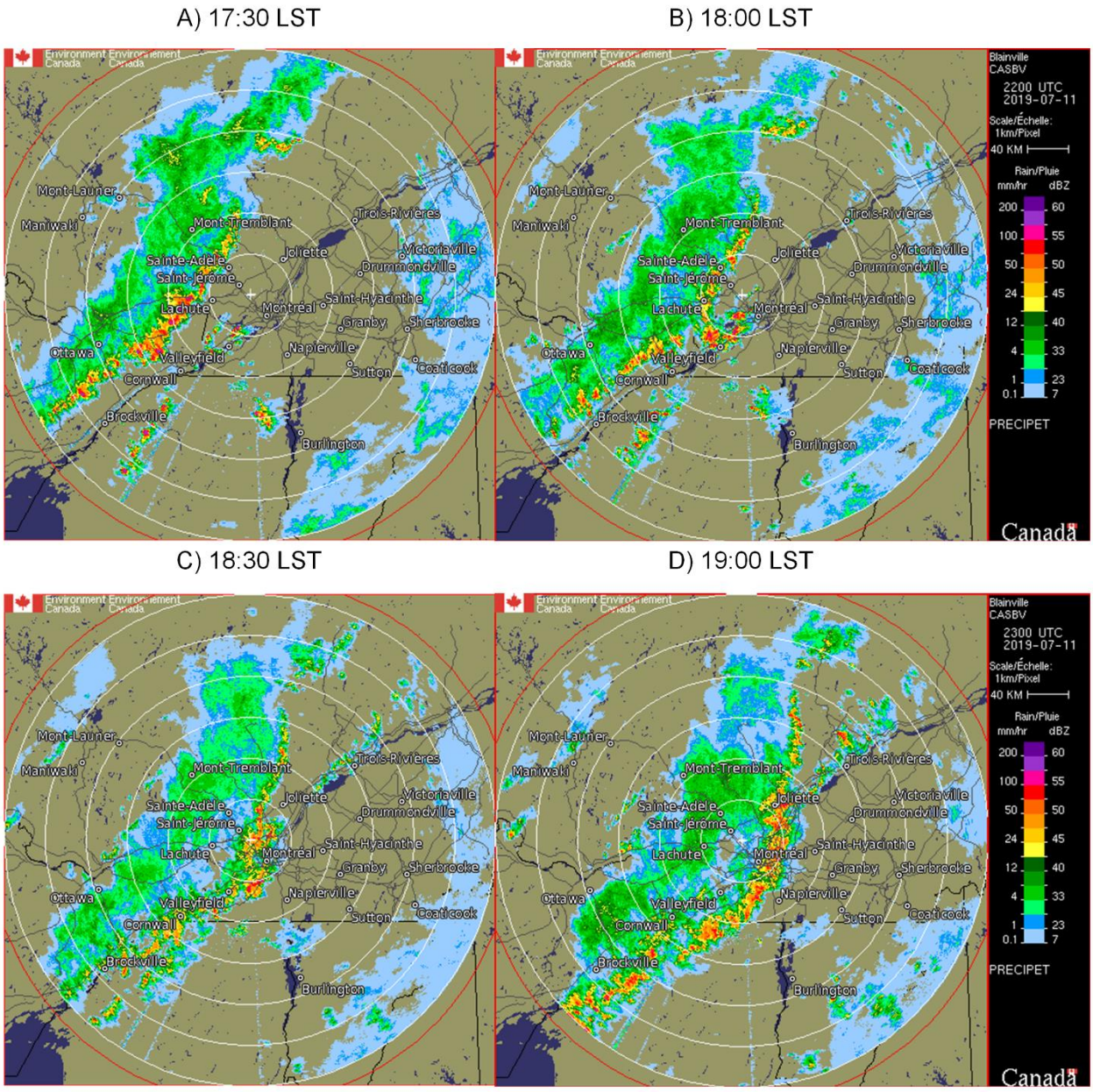

Figure C.1. **Radar images for the SQUALL event.** Radar images from the Blainville radar on 2019-07-12 at a) 1730 LST (2130 UTC), b) 1800 LST (2200 UTC), c) 1830 LST (2230 UTC) and d) 1900 LST (2300 UTC). The island of Montreal is located southeast from the center of the radar (see label).

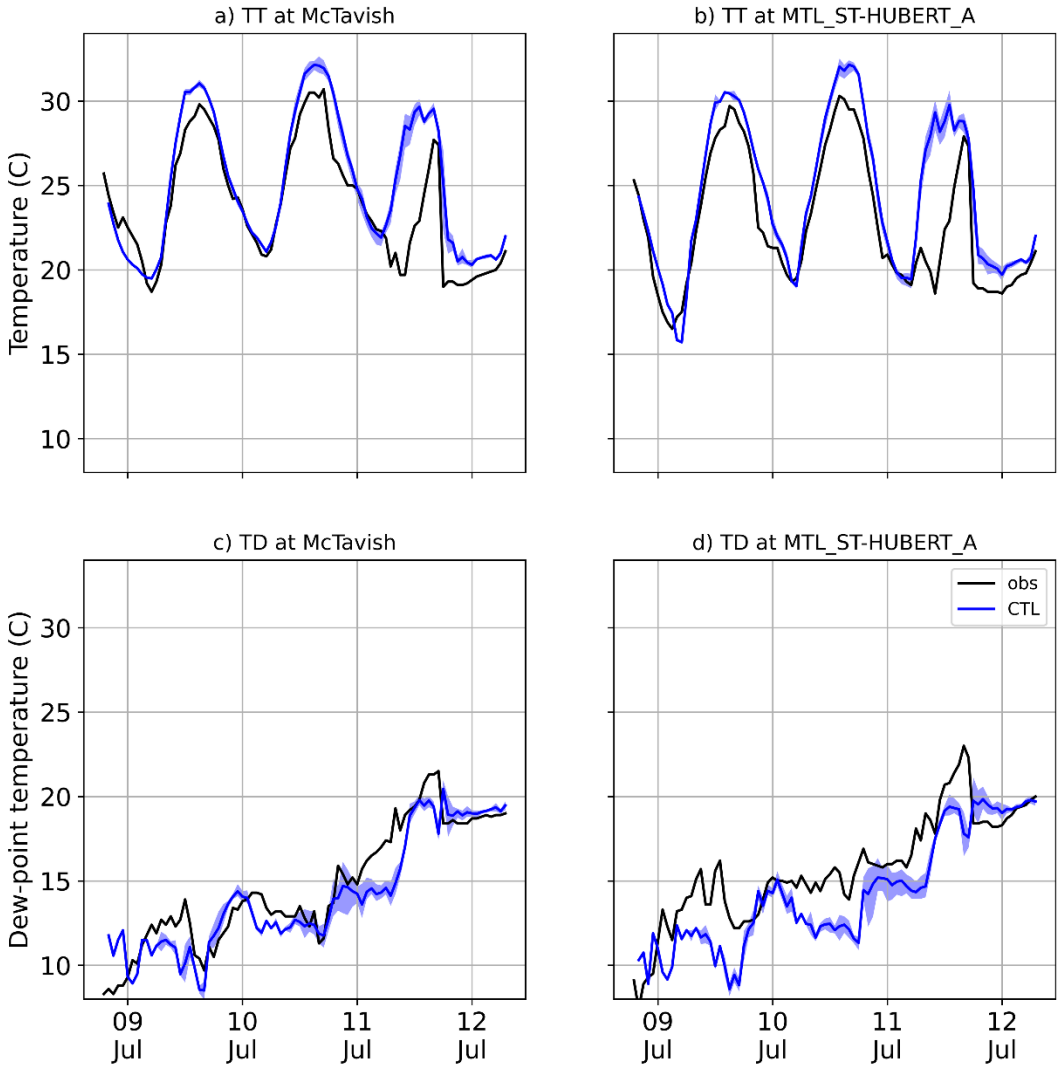

Figure C.2. **Timeseries of observed and simulated surface variables for the SQUALL event.** Same as Fig 1.7, but for the 2019 event. Observed (black) and simulated (blue) surface temperature (TT, a and b) and dew point temperature (TD, c and d) at station McTavish (WTA, a and c) and St-Hubert (YHU, b and d) for the SQUALL event. The blue shading shows the ensemble spread.

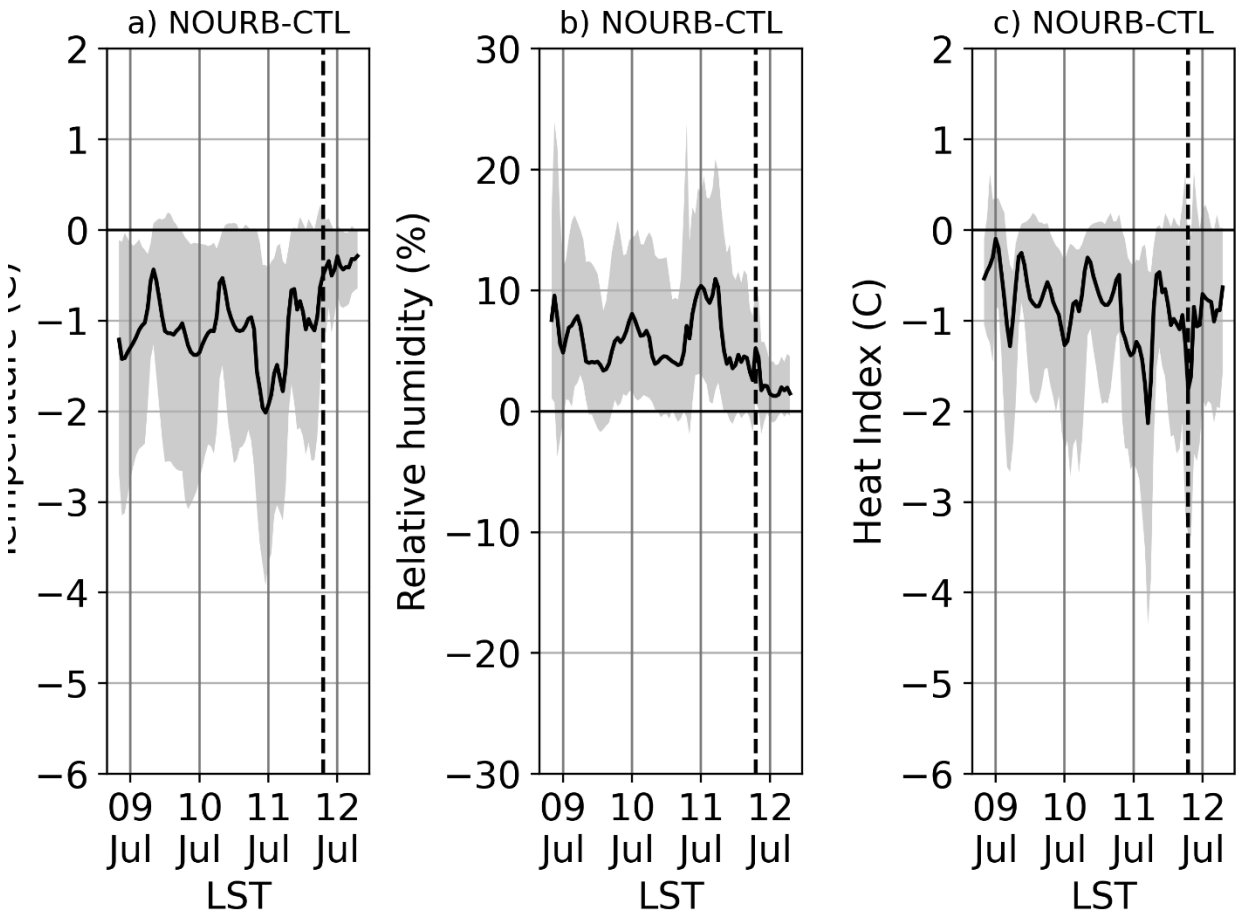

Figure C.3. **Changes in averaged surface temperature, relative humidity and heat index for the SQUALL event.** Spatial timeseries of the difference in surface temperature (a), relative humidity (b) and heat index (c) between NOURB-CTL model runs for the 2019 event. The black line is the spatial average on the island of Montreal of the difference between the sensitivity and the CTL experiments. The gray area is the 5th to 95th percentile and represents the spatial variability on the island of Montreal. Vertical lines show 00:00 local time.

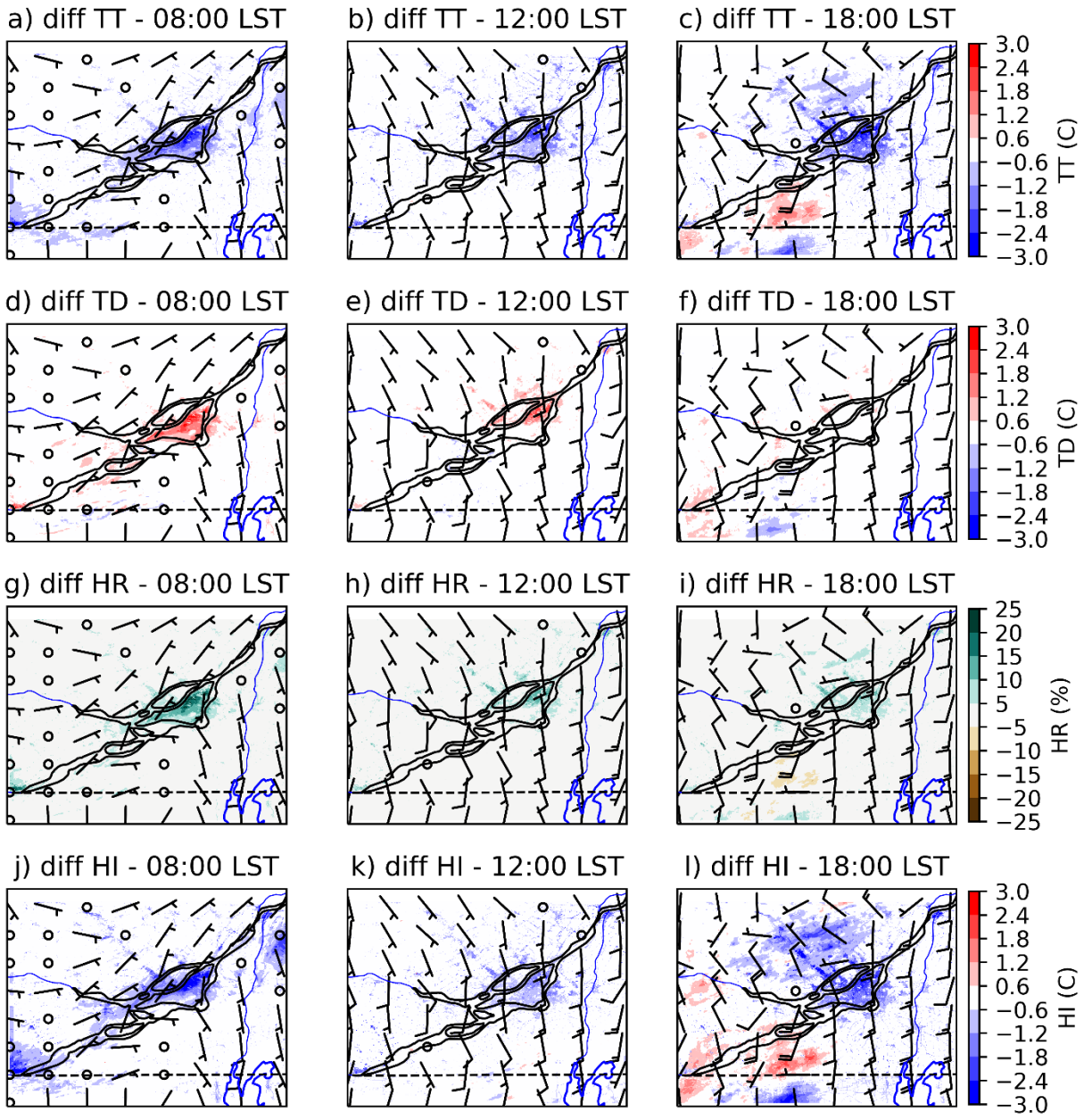

Figure C.4. **Changes in surface temperature, dew point, relative humidity and heat index between NOURB and CTL for the SQUALL event.** Same as Fig 1.12, but for the 2019 event. Anomalies in air temperature (a, b, c), dew-point temperature (d, e, f), relative humidity (g, h, i) and heat index (j, k, l) between NOURB and CTL experiments. The three columns correspond to different times: 2019-07-11 08:00 LST (left), 2019-07-11 12:00 LST (center) and 2019-07-11 18:00 LST (right). Surface winds for the CTL experiment are shown (in knots).

BIBLIOGRAPHIE

Anderson, G. B., Bell, M. L., & Peng, R. D. (2013). Methods to Calculate the Heat Index as an Exposure Metric in Environmental Health Research. *Environmental Health Perspectives*, *121*(10), 1111–1119. https://doi.org/10.1289/ehp.1206273

Bélair, S., Crevier, L.-P., Mailhot, J., Bilodeau, B., & Delage, Y. (2003). Operational Implementation of the ISBA Land Surface Scheme in the Canadian Regional Weather Forecast Model. Part I: Warm Season Results. *Journal of Hydrometeorology*, *4*(2), 352–370. https://doi.org/10.1175/1525-7541(2003)4<352:OIOTIL>2.0.CO;2

Bélair, S., Leroyer, S., Seino, N., Spacek, L., Souvanlassy, V., & Paquin-Ricard, D. (2018). Role and Impact of the Urban Environment in a Numerical Forecast of an Intense Summertime Precipitation Event over Tokyo. *気象集誌. 第2 輯*, *advpub*, 2018–011. https://doi.org/10.2151/jmsj.2018-011

Berardi, U., Jandaghian, Z., & Graham, J. (2020). Effects of greenery enhancements for the resilience to heat waves: A comparison of analysis performed through mesoscale (WRF) and microscale (Envi-met) modeling. *Science of The Total Environment*, *747*, 141300. https://doi.org/10.1016/j.scitotenv.2020.141300

Bornstein, R., & Lin, Q. (2000). Urban heat islands and summertime convective thunderstorms in Atlanta: Three case studies. *Atmospheric Environment*, *34*(3), 507–516. https://doi.org/10.1016/S1352-2310(99)00374-X

Broadbent, A. M., Coutts, A. M., Tapper, N. J., & Demuzere, M. (2018). The cooling effect of irrigation on urban microclimate during heatwave conditions. *Urban Climate*, *23*, 309–329. https://doi.org/10.1016/j.uclim.2017.05.002

Carrera, M. L., Gyakum, J. R., & Lin, C. A. (2009). Observational Study of Wind Channeling within the St. Lawrence River Valley. *Journal of Applied Meteorology and Climatology*, *48*(11), 2341–2361. https://doi.org/10.1175/2009JAMC2061.1

Côté, J., Gravel, S., Méthot, A., Patoine, A., Roch, M., & Staniforth, A. (1998). The Operational CMC–MRB Global Environmental Multiscale (GEM) Model. Part I: Design Considerations and Formulation. *Monthly Weather Review*, *126*(6), 1373–1395. https://doi.org/10.1175/1520-0493(1998)126<1373:TOCMGE>2.0.CO;2

Dookhie, G. C. (2011). *Dynamics of heavy warm-season precipitation events in Montréal* [Master of Science]. McGill University.

Erell, E., Pearlmutter, D., Boneh, D., & Kutiel, P. B. (2014). Effect of high-albedo materials on pedestrian heat stress in urban street canyons. *Urban Climate*, *10*, 367–386. https://doi.org/10.1016/j.uclim.2013.10.005

Fortin, V., Roy, G., Stadnyk, T., Koenig, K., Gasset, N., & Mahidjiba, A. (2018). Ten Years of Science Based on the Canadian Precipitation Analysis: A CaPA System Overview and Literature Review. *Atmosphere-Ocean*, *56*(3), 178–196. https://doi.org/10.1080/07055900.2018.1474728

He, B.-J., Ding, L., & Prasad, D. (2020). Wind-sensitive urban planning and design: Precinct ventilation performance and its potential for local warming mitigation in an open midrise gridiron precinct. *Journal of Building Engineering*, *29*, 101145. https://doi.org/10.1016/j.jobe.2019.101145

Herrmann, J., & Matzarakis, A. (2012). Mean radiant temperature in idealised urban canyons—Examples from Freiburg, Germany. *International Journal of Biometeorology*, *56*(1), 199–203. https://doi.org/10.1007/s00484-010-0394-1

Honnert, R., Efstathiou, G. A., Beare, R. J., Ito, J., Lock, A., Neggers, R., Plant, R. S., Shin, H. H., Tomassini, L., & Zhou, B. (2020). The Atmospheric Boundary Layer and the “Gray Zone” of Turbulence: A

Critical Review. *Journal of Geophysical Research: Atmospheres*, *125*(13). https://doi.org/10.1029/2019JD030317

Huong, H. T. L., & Pathirana, A. (2013). Urbanization and climate change impacts on future urban flooding in Can Tho city, Vietnam. *Hydrology and Earth System Sciences*, *17*(1), 379–394. https://doi.org/10.5194/hess-17-379-2013

Husain, S. Z., & Girard, C. (2017). Impact of Consistent Semi-Lagrangian Trajectory Calculations on Numerical Weather Prediction Performance. *Monthly Weather Review*, *145*(10), 4127–4150. https://doi.org/10.1175/MWR-D-17-0138.1

Krayenhoff, E. S., Jiang, T., Christen, A., Martilli, A., Oke, T. R., Bailey, B. N., Nazarian, N., Voogt, J. A., Giometto, M. G., Stastny, A., & Crawford, B. R. (2020). A multi-layer urban canopy meteorological model with trees (BEP-Tree): Street tree impacts on pedestrian-level climate. *Urban Climate*, *32*, 100590. https://doi.org/10.1016/j.uclim.2020.100590

Krayenhoff, E. S., & Voogt, J. A. (2010). Impacts of Urban Albedo Increase on Local Air Temperature at Daily–Annual Time Scales: Model Results and Synthesis of Previous Work. *Journal of Applied Meteorology and Climatology*, *49*(8), 1634–1648. https://doi.org/10.1175/2010JAMC2356.1

Kundzewicz, Z. W., Pińskwar, I., & Brakenridge, G. R. (2013). Large floods in Europe, 1985–2009. *Hydrological Sciences Journal*, *58*(1), 1–7. https://doi.org/10.1080/02626667.2012.745082

Lee, H., Mayer, H., & Chen, L. (2016). Contribution of trees and grasslands to the mitigation of human heat stress in a residential district of Freiburg, Southwest Germany. *Landscape and Urban Planning*, *148*, 37–50. https://doi.org/10.1016/j.landurbplan.2015.12.004

Lemonsu, A., Belair, S., & Mailhot, J. (2009). The New Canadian Urban Modelling System: Evaluation for Two Cases from the Joint Urban 2003 Oklahoma City Experiment. *Boundary-Layer Meteorology*, *133*(1), 47–70. https://doi.org/10.1007/s10546-009-9414-2

Lemonsu, A., Masson, V., Shashua-Bar, L., Erell, E., & Pearlmutter, D. (2012). Inclusion of vegetation in the Town Energy Balance model for modelling urban green areas. *Geoscientific Model Development*, *5*(6), 1377–1393. https://doi.org/10.5194/gmd-5-1377-2012

Leroyer, S., Bélair, S., Alavi, N., Munoz-Alpizar, R., Nikiema, O., & Popadic, I. (2019). *Influence des aménagements du tissu urbain sur la micro-météorologie et le confort thermique: Cas des villes de Montréal et Toronto*. Zenodo. https://doi.org/10.5281/zenodo.7324545

Leroyer, S., Bélair, S., Souvanlasy, V., Vallée, M., Pellerin, S., & Sills, D. (2022). Summertime Assessment of an Urban-Scale Numerical Weather Prediction System for Toronto. *Atmosphere*, *13*(7), 1030. https://doi.org/10.3390/atmos13071030

Li, Y., Fowler, H. J., Argüeso, D., Blenkinsop, S., Evans, J. P., Lenderink, G., Yan, X., Guerreiro, S. B., Lewis, E., & Li, X. (2020). Strong Intensification of Hourly Rainfall Extremes by Urbanization. *Geophysical Research Letters*, *47*(14). https://doi.org/10.1029/2020GL088758

Liu, J., & Niyogi, D. (2019). Meta-analysis of urbanization impact on rainfall modification. *Scientific Reports*, *9*(1), 7301. https://doi.org/10.1038/s41598-019-42494-2

Macdonald, R. W., Griffiths, R. F., & Hall, D. J. (1998). An improved method for the estimation of surface roughness of obstacle arrays. *Atmospheric Environment*, *32*(11), 1857–1864. https://doi.org/10.1016/S1352-2310(97)00403-2

Madsen, H., Lawrence, D., Lang, M., Martinkova, M., & Kjeldsen, T. R. (2014). Review of trend analysis and climate change projections of extreme precipitation and floods in Europe. *Journal of Hydrology*, *519*, 3634–3650. https://doi.org/10.1016/j.jhydrol.2014.11.003

Martilli, A., Krayenhoff, E. S., & Nazarian, N. (2020). Is the Urban Heat Island intensity relevant for heat mitigation studies? *Urban Climate*, *31*, 100541. https://doi.org/10.1016/j.uclim.2019.100541

Mason, P. J., & Brown, A. R. (1999). On Subgrid Models and Filter Operations in Large Eddy Simulations. *Journal of the Atmospheric Sciences*, *56*(13), 2101–2114. https://doi.org/10.1175/1520-0469(1999)056<2101:OSMAFO>2.0.CO;2

Masson, V. (2000). A Physically-Based Scheme For The Urban Energy Budget In Atmospheric Models. *Boundary-Layer Meteorology*, *94*(3), 357–397. https://doi.org/10.1023/A:1002463829265

Milbrandt, J. A., & Yau, M. K. (2005). A Multimoment Bulk Microphysics Parameterization. Part I: Analysis of the Role of the Spectral Shape Parameter. *Journal of the Atmospheric Sciences*, *62*(9), 3051–3064. https://doi.org/10.1175/JAS3534.1

Miller, J. D., & Hutchins, M. (2017). The impacts of urbanisation and climate change on urban flooding and urban water quality: A review of the evidence concerning the United Kingdom. *Journal of Hydrology: Regional Studies*, *12*, 345–362. https://doi.org/10.1016/j.ejrh.2017.06.006

Mills, G. (2008). Luke Howard and The Climate of London. *Weather*, *63*(6), 153–157. https://doi.org/10.1002/wea.195

Niyogi, D., Pyle, P., Lei, M., Arya, S. P., Kishtawal, C. M., Shepherd, M., Chen, F., & Wolfe, B. (2011). Urban Modification of Thunderstorms: An Observational Storm Climatology and Model Case Study for the Indianapolis Urban Region. *Journal of Applied Meteorology and Climatology*, *50*(5), 1129–1144. https://doi.org/10.1175/2010JAMC1836.1

Noilhan, J., & Planton, S. (1989). A Simple Parameterization of Land Surface Processes for Meteorological Models. *Monthly Weather Review*, *117*(3), 536–549. https://doi.org/10.1175/1520-0493(1989)117<0536:ASPOLS>2.0.CO;2

Oke, T. R. (1981). Canyon geometry and the nocturnal urban heat island: Comparison of scale model and field observations. *Journal of Climatology*, *1*(3), 237–254. https://doi.org/10.1002/joc.3370010304

Oke, T. R. (1982). The energetic basis of the urban heat island. *Quarterly Journal of the Royal Meteorological Society*, *108*(455), 1–24.

Oke, T. R., & Maxwell, G. B. (1975). Urban heat island dynamics in Montreal and Vancouver. *Atmospheric Environment (1967)*, *9*(2), 191–200. https://doi.org/10.1016/0004-6981(75)90067-0

Oke, T. R., Mills, G., Christen, A., & Voogt, J. A. (2017). *Urban Climates*. Cambridge University Press.

Ouellette-Vézina, H. (2022, May 24). Orages violents: La province victime d'un… derecho. *La Presse*. https://www.lapresse.ca/actualites/2022-05-24/orages-violents/la-province-victime-d-un-derecho.php

Redon, E. C., Lemonsu, A., Masson, V., Morille, B., & Musy, M. (2017). Implementation of street trees within the solar radiative exchange parameterization of TEB in SURFEX v8.0. *Geoscientific Model Development*, *10*(1), 385–411. https://doi.org/10.5194/gmd-10-385-2017

Shepherd, J. M. (2013). Impacts of urbanization on precipitation and storms: Physical insights and vulnerabilities. *Climate Vulnerability*, *5*, 109–125.

Stewart, I. D. (2011). *Redifining the urban heat island* [Thesis]. University of British Columbia.

Taha, H., Akbari, H., Rosenfeld, A., & Huang, J. (1988). Residential cooling loads and the urban heat island—The effects of albedo. *Building and Environment*, *23*(4), 271–283. https://doi.org/10.1016/0360-1323(88)90033-9

Taleghani, M., & Berardi, U. (2018). The effect of pavement characteristics on pedestrians' thermal comfort in Toronto. *Urban Climate*, *24*, 449–459. https://doi.org/10.1016/j.uclim.2017.05.007

Teufel, B., Sushama, L., Huziy, O., Diro, G. T., Jeong, D. I., Winger, K., Garnaud, C., de Elia, R., Zwiers, F. W., Matthews, H. D., & Nguyen, V.-T.-V. (2019). Investigation of the mechanisms leading to the 2017 Montreal flood. *Climate Dynamics*, *52*(7), 4193–4206. https://doi.org/10.1007/s00382-018-4375-0

Trenberth, K. E. (2011). Changes in precipitation with climate change. *Climate Research*, *47*(1–2), 123–138. https://doi.org/10.3354/cr00953

Wang, Y., & Akbari, H. (2016). The effects of street tree planting on Urban Heat Island mitigation in Montreal. *Sustainable Cities and Society*, *27*, 122–128. https://doi.org/10.1016/j.scs.2016.04.013

World Meteorological Organization (WMO). (2018). *Guide to Instruments and Methods of Observation (WMO-No. 8)* (2018th and 2021 editions ed.). WMO.

World urbanization prospects: The 2018 revision. (2019). United Nations.

Yang, F., Lau, S. S. Y., & Qian, F. (2011). Thermal comfort effects of urban design strategies in high-rise urban environments in a sub-tropical climate. *Architectural Science Review*, *54*(4), 285–304. https://doi.org/10.1080/00038628.2011.613646

Yang, J., Wang, Z.-H., Kaloush, K. E., & Dylla, H. (2016). Effect of pavement thermal properties on mitigating urban heat islands: A multi-scale modeling case study in Phoenix. *Building and Environment*, *108*, 110–121. https://doi.org/10.1016/j.buildenv.2016.08.021

Zhang, Y., Miao, S., Dai, Y., & Bornstein, R. (2017). Numerical simulation of urban land surface effects on summer convective rainfall under different UHI intensity in Beijing: Urban Effects on Rainfall in Beijing. *Journal of Geophysical Research: Atmospheres*, *122*(15), 7851–7868. https://doi.org/10.1002/2017JD026614